Distribution Agreement

In presenting this thesis as a partial fulfillment of the requirements for a degree from Emory University, I hereby grant to Emory University and its agents the non-exclusive license to archive, make accessible, and display my thesis in whole or in part in all forms of media, now or hereafter now, including display on the World Wide Web. I understand that I may select some access restrictions as part of the online submission of this thesis. I retain all ownership rights to the copyright of the thesis. I also retain the right to use in future works (such as articles or books) all or part of this thesis.

Charlene Chan April 17, 2012

Photoreleasable dynamic interfaces to control hybrid cell-supported lipid membrane junctions

by

Charlene Chan

Dr. Khalid Salaita
Adviser

Department of Chemistry

Dr. Khalid Salaita

Adviser

Dr. Stefan Lutz

Committee Member

Dr. Keith Berland

Committee Member

2012

Photoreleasable dynamic interfaces to control hybrid cell-supported lipid membrane junctions

By

Charlene Chan

Dr. Khalid Salaita

Adviser

An abstract of
a thesis submitted to the Faculty of Emory College of Arts and Sciences
of Emory University in partial fulfillment
of the requirements of the degree of
Bachelor of Sciences with Honors

Department of Chemistry

2012

Abstract

Photoreleasable dynamic interfaces to control cell-supported lipid membrane junctions

By Charlene Chan

Cells typically respond to the chemical and physical properties of their environment through membrane receptors. One challenge in this area pertains to investigating receptor response to the physical properties of a signaling ligand *in situ.* Herein, we describe the development of a photoactivatable platform to dynamically control the immobilization of biomolecules to a supported lipid membrane with high spatial and temporal resolution. This system employs photocleavable DNA tethers that are easily multiplexed and labeled with ligands of interest to selectively release anchored biomolecules from a lipid membrane surface. Biotin-streptavidin anchoring chemistry is used to incorporate oligonucleotide capture strands that are functionalized with a 5'-2-nitrophenyl group into the membrane. These strands are complementary to cyclic Arg-Gly-Asp (cRGD) peptides conjugated oligonucleotides that engage adhesion receptors in cells, and can be released upon photo-irradiation. We describe the synthesis and properties of these model membranes and their potential use in studying dynamic cell adhesions.

Photoreleasable dynamic interfaces to control cell-supported lipid membrane junctions

By

Charlene Chan

Dr. Khalid Salaita

Adviser

A thesis submitted to the Faculty of Emory College of Arts and Sciences
of Emory University in partial fulfillment
of the requirements of the degree of
Bachelor of Sciences with Honors

Department of Chemistry

2012

Acknowledgements

To the Department of Chemistry, thank you for showing me the difference between declaring a major and belonging to a department. It has been a great honor and pleasure to be part of such an amazing community.

To the members of the Salaita lab, thank you for all the support and guidance over the years. In particular, to Yoshie Narui and Kevin Yehl, thank you for all the times I interrupted you with questions, frustrations and coffee breaks.

To my committee members, thank you for your time, patience, and comments. I learned a lot about being a better scientist.

To Dr. Khalid Salaita, thank you for replying to my email that fateful September day and for everything since then. Doing research has been a fulfilling and frustrating experience, but I am glad that I had you as an advisor to challenge and encourage me.

Table of Contents

List of Figures and Tables

Background

Cell fate is regulated by external physical and chemical signals from the surrounding environment.[1] Receptor proteins embedded in the cell membrane receive these extrinsic signals and relay the information to the rest of the cell by initiating coordinated cascades of biochemical events, which subsequently influence the activity of genes and proteins.[2] One of the primary receptors responsible for sensing and transmitting physical signals is the integrin family of receptors.[3] The following section describes the integrin receptors and some common methods to investigate their biochemical and biophysical properties.

Integrin receptors

Integrins are a family of over 20 heterodimeric glycoprotein receptors, comprised of a pair of non-covalently linked *α*- and *β*-subunits.[4] Each subunit has a large extracellular domain and a short cytoplasmic domain, and spans the cell membrane only once.[4a] The extracellular domain engages with the external environment and recognizes ligands of the extracellular matrix (ECM), while the cytoplasmic tail helps coordinate intracellular reaction cascades and binding to the cell cytoskeleton.[4a, 5] Integrins chemically recognize external motifs such as Arg-Gly-Asp (RGD) found within ECM proteins such as fibronectin.[1b, 6] Although integrins can bind to both soluble and anchored ligands, the chemical response of integrins depends on the physical nature of the ligand.[4a] For example, interactions between the integrin receptors and anchored ligands on rigid surfaces form local focal adhesions and generate force, in contrast to soluble ligands that can be used as cancer therapeutics.[3-4, 7] These receptors play important roles in mediating dynamic cell-matrix and cell-cell interactions, and are critical for cell adhesion and cell migration.[4a, 5]

Stimulus-responsive cell adhesive substrates

In order to study chemo-mechanical coupling in integrins and its influence on cell behavior, model systems have been developed to mimic *in vivo* cell-matrix and cell-cell

interactions.[1] In general, these systems immobilize a cell adhesive moiety to a substrate and render the substrate responsive to external stimuli using a variety of modification techniques and anchoring chemistry. One common cell recognition motifs for cell adhesion is the Arg-Gly-Asp (RGD) peptide sequence, which can serve as a minimal adhesion peptide, and can primarily interact with $\alpha_v\beta_3$ integrin receptors.[6] The ability of these substrates to respond to an external stimulus allows for dynamic control over the cell adhesion properties of these substrates, and a better understanding of chemo-mechanical coupling across integrins.[1a] Incorporating external control into cell adhesive substrates is not only important for studying the influence of focal adhesions in cell behavior, such as cell migration in wound healing, development and cancer metastasis, but also for designing tissue engineering and cell culture substrates.[1a, 6]

One powerful approach to control cell adhesive properties on such substrates requires photochemical stimuli, which switch the substrate between adhesive and non-adhesive states. For example, Auernhiemer *et al.*[8] tethered cyclic RGD to polymethyl methacrylate (PMMA) surfaces using an acrylamide anchor with a photoswitchable diazobenzene spacer. The diazobenzene group photoisomerized between its *cis* and *trans* isomers upon irradiation with light at 366 nm and 450 nm, respectively, which subsequently influenced the distance and the orientation of the cRGD peptide to the surface and to the integrin receptor (Figure 1).[8] More stable cell adhesion was observed for surfaces irradiated with 450nm light, as higher affinity receptor-ligand interactions were possible when the linker was in its *trans* isomer.[8]

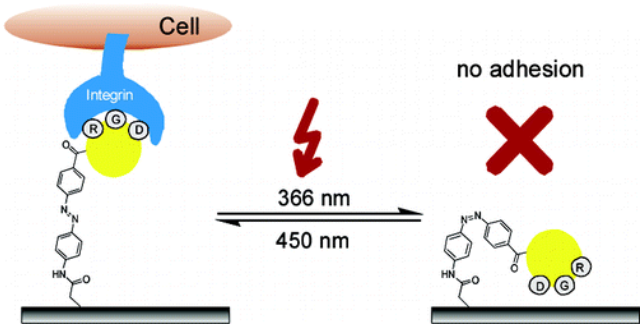

Figure 1 : Photoisomerization of the diazobenzene group changes RGD peptide-integrin interactions. (Adapted from ref. 8 with permission. Copyright © 2005 American Chemical Society)

In another example, Nakanishi *et al.*[9] functionalized glass substrates with an alkylsiloxane monolayer displaying a photocleavable 2-nitrobenzyl group. In this system, non-adhesive bovine serum albumin (BSA) was allowed to adsorb onto the monolayer via hydrophobic interactions between the protein and the 2-nitrobenzyl groups, thereby inhibiting cell adhesion (Figure 2). Upon irradiation with ultraviolet light, the 2-nitrobenzyl groups photocleaved, resulting in an increase in the hydrophilicity of the surface and the corresponding dissociation of BSA from the surface. Fibronectin, a component of the extracellular matrix, could then adsorb to the carboxylic acids displayed by the monolayer and render the surface cell adhesive.[9] Cell migration was controlled in a similar manner by rendering a region alongside a cell to become more adhesive.[10] Wirkner *et al.* [11] utilized photocleavable linkers containing an intercalated 4,5,-dialkoxy 1-(2-nitrophenyl)-ethyl group to anchor RGD peptides to gold-coated surfaces. Human umbilical vascular endothelial cells (HUVECs) attached and spread on theses functionalized substrates. However, cells rounded up and detached when the surfaces were irradiated and the photolabile group cleaved. More recently, light sensitive three-dimensional cellular environments that can alter cell adhesion and promote differentiation have also been developed. For example, Kloxin *et al.*[12] encapsulated human mesenchymal stem cells (hMSCs) in hydrogels containing photodegradable acrylate coupled to linear RGD peptides. Upon irradiation, the peptide was released and diffused out of the gel. hMSCs encapsulated in these irradiated hydrogels up-regulated glycosaminoglycan and type II collagen, indicating chondrogenic differentiation.[12]

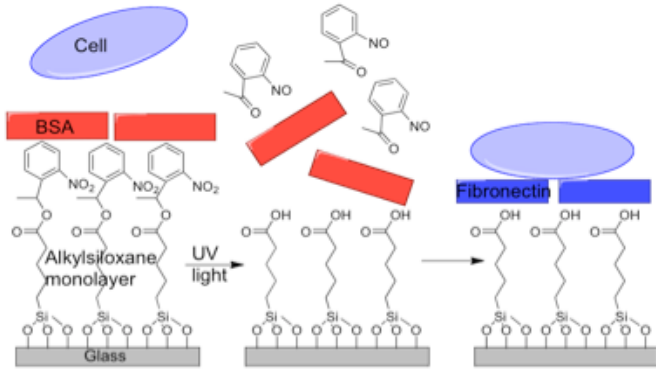

Figure 2: Scheme of a stimulus-responsive cell adhesive surface. UV irradiation changes the properties of the surface from inhibiting cell adhesion to promoting cell adhesion. (Adapted from ref. 9 with permission. Copyright © 2004 American Chemical Society)

A second class of techniques to control ligands and the cell adhesive properties of substrates involve electrochemical input. For example, Wildt *et al.*[13] developed programmed subcellular release, which involved tethering RGD peptides onto an array for gold lines on a chip-like device through thiol linkages (Figure 3). When a low-voltage pulse was run through an individual gold line, the peptides were released. This caused a portion of the cell to detach from the surface, resulting in cell contraction.[13] Raghavan *et al.*[14] applied a double microcontact printing approach to pattern gold substrates with permanently cell-nonadhesive, permanently cell-adhesive and switchable regions. By taking advantage of different reduction potentials, a region patterned with a polyethylene glycol (PEG) terminated self-assembled monolayer (SAM) could be selectively desorbed and rendered cell-adhesive, while a region patterned with a methyl-terminated SAM remained after application of a -1000 mV voltage.[14] Cells would spread from the permanently cell-adhesive regions to the switched regions.

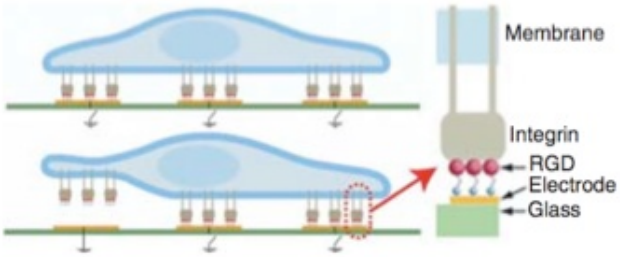

Figure 3: Schematic of programmed subcellular release. (Adapted from ref. 13b with permission. Copyright © 2010, Nature Publishing Group)

While these stimulus-responsive cell adhesive substrates allow for some external control over cell adhesion and cell migration, they are not sufficient for the study of chemo-mechanical coupling across integrins. Because the cell adhesive moieties are immobilized to the substrates, the dynamics of ligand-receptor complexes and any subsequent organization, polyvalency and mechanical strain are not reconstituted. The influence of the physical properties of these ligand-receptor complexes can be better explored using a dynamic and fluid surface.

Studying receptor-ligand interactions with supported lipid bilayers

Although stimulus-responsive substrates are effective tools to study cell adhesion and migration, they do not adequately reflect the dynamic nature of biological membranes and bio-interfaces. Not only can biological membranes change lateral organization and curvature to mediate signaling and transport, the constituent lipids and proteins can also aggregate to form supramolecular structures that influence cell transduction and behavior.[2a] One strategy employs supported lipid bilayers, which are model membranes on solid substrates whose surfaces can be functionalized with biomolecules of interest.[15] These bilayers are fluid and allow for the lateral diffusion of the phospholipids and displayed biomolecules, thereby recapitulating the two-dimensional dynamic nature of biological membranes.[2a, 15b] This allows a cell interacting with the membrane to spatially organize the displayed ligands at the hybrid cell-cell interface. Thus, these model membranes can be used to study the effects of physical inputs and spatiotemporal organization on receptor-ligand interactions and their functions. For example, Salaita *et al.*[16] demonstrated that introducing physical barriers to EphA2 receptor tyrosine kinase clustering changes breast cancer cells' response to the ligand, ephrin-A1. Recently, Sheetz[4b] and colleagues functionalized supported lipid bilayers with cyclic RGD ligands to investigate spatial organization of activated integrins. They showed that early integrin clustering aided in the recruitment of adhesion proteins and activated actin polymerization.

However, one limitation of the current supported lipid bilayer systems is the inability to encode multiple ligands on a surface. These model systems rely on only a few methods of anchoring chemistry, such as biotin-streptavidin affinity anchoring chemistry and non-covalent interactions, to functionalize surfaces. These methods of anchoring chemistry restrict the number of different ligands that can be displayed on the membrane, as these interactions cannot be programmed for any specific ligand.

Lipid-oligonucleotide conjugates

One strategy to encode both dynamic assembly and recognition into model membranes involves lipid-oligonucleotide conjugates. These amphiphilic molecules consist of a hydrophilic oligonucleotide linked to a hydrophobic moiety such as a lipid tail or a cholesterol derivative.[17] The oligonucleotide head allows information to be encoded due to DNA's ability to recognize its complementary strand and other substrates, while the lipid tail confers aggregation and assembly properties.[17]

These properties make lipid-oligonucleotide conjugates attractive for model systems. For example, Boxer and colleagues[18] studied the mechanisms of membrane fusion and rearrangement of vesicle fusion by modeling the interactions of the SNARE protein complex with vesicles tethered to supported lipid membranes that use DNA-lipid conjugates (Figure 4). Tethered vesicles fused only when another pair of complementary DNA strands hybridized and docked the vesicles together.[18] Furthermore, Loew *et al.*[19] developed conjugates consisting of peptide nucleic acid (PNA) and DNA with differing hydrophobic moieties, which preferentially partitioned into the liquid-ordered and liquid-disordered domains of heterogeneous giant unilamellar vesicles. The domain-specific partitioning could be controlled using temperature, resulting in the intermixing and separation of lipid-oligonucleotide conjugates at high and low

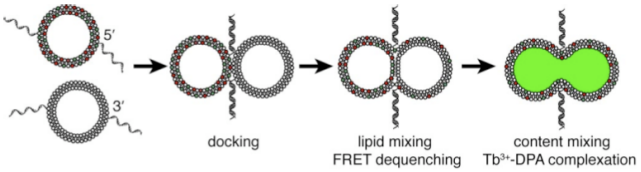

Figure 4 : Schematic of vesicle fusion assisted by DNA hybridization. (Adapted from ref 18 with permission. Copyright © 2009, the National Academy of Sciences of the United States of America)

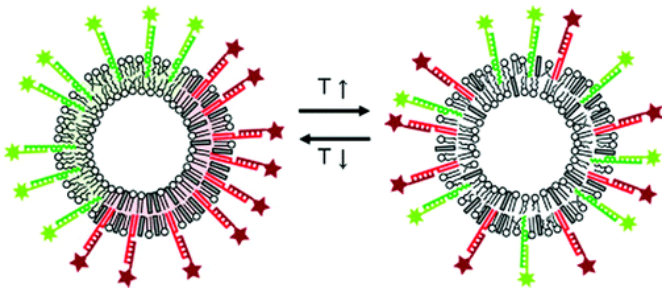

Figure 5: Temperature controlled domain-partitioning of lipid-oligonucleotide conjugates. (Adapted from ref 19 with permission. Copyright © 2010, American Chemical Society)

temperatures, respectively (Figure 5).[19] The domain partitioning modeled lipid rafts, which can then be visualized using complementary fluorescently labeled DNA strands[19]. Moreover, these amphiphilic molecules and their role as potential programmable soft nanomaterials have been recently investigated. For example, Gianneschi and colleagues[20] developed stimuli-responsive liposomes, of which the morphology of the lipid-oligonucleotide aggregates reversibly switch from unilamellar vesicles with a bilayer structure to smaller micelles with a monolayer structure using DNA hybridization. The change from single-stranded DNA to duplex DNA of the oligonucleotide polar head led to an increase in steric and electronic repulsion, resulting in the vesicle-micelle phase shift.[20]

Innovation

Herein, we describe a novel self-healing and dynamic stimulus-responsive substrate. This substrate is a photoactivatable supported lipid bilayer that allows for the controlled release of immobilized biomolecules with high spatial and temporal resolution. Unlike previously described ligand-presenting surfaces, this substrate employs photocleavable DNA tethers to anchor and then selectively release biomolecules from a supported lipid bilayer; this light sensitive lipid membrane platform combines the utility of dynamic cell adhesive substrates and the programmability of lipid-DNA conjugates. The design strategy involves the immobilization ligand molecules functionalized with single-stranded oligonucleotides to a supported lipid bilayer displaying the complementary capture strands (Figure 6). To simplify the development of the system, the capture strands are incorporated into the membrane using biotin-streptavidin affinity anchoring chemistry instead of being true lipid oligonucleotide conjugates. The capture oligonucleotide strands are functionalized with a photosensitive 5'-modified 2-nitrophenyl phosphoramidite. Upon irradiation with ultraviolet light, the nitrophenyl group forms radicals and quenches through rearrangement, resulting in a photocleavage event. Due to the positioning of

this UV-active functional group at the 5' terminus of the capture oligonucleotide, the photocleavage event releases the oligonucleotide and any tethered ligand molecules into solution, while the biotinyl-2-nitrosoacetophenone derivative remains on the surface (Figure 7).[21] Importantly, the lateral fluidity of the membrane will then allow for recovery of the released ligand.

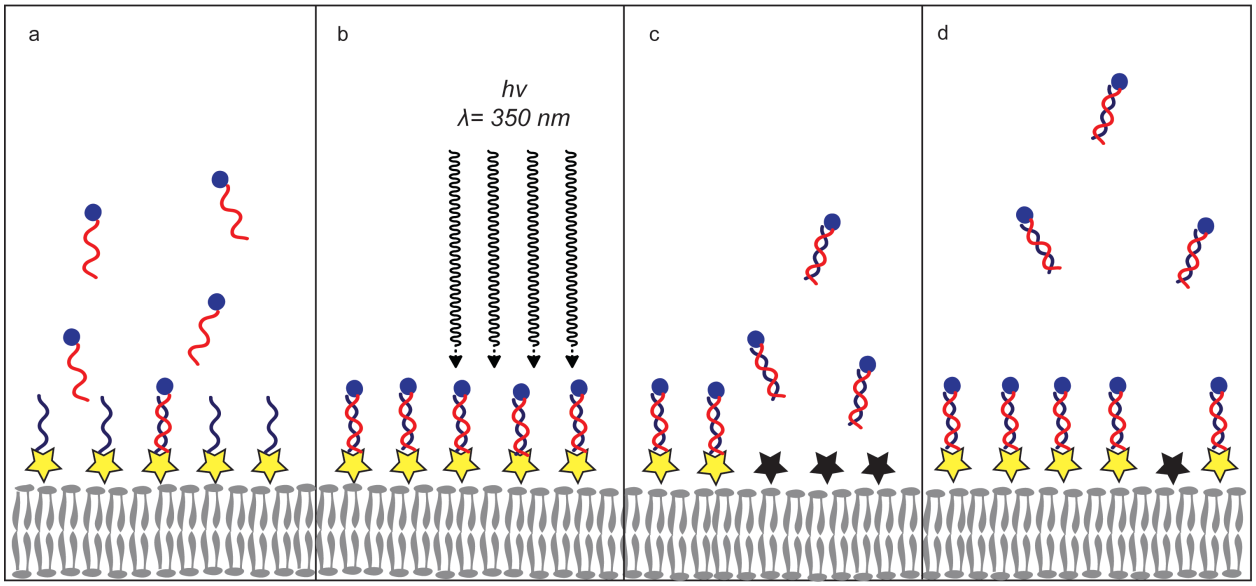

Figure 6: Schematic of the dynamic photoactivatable synthetic cell surface that uses DNA tethers to immobilize peptides onto a supported lipid bilayer. a) The synthetic cell surface is comprised of a lipid bilayer (gray two-tailed representative phospholipids) displaying oligonucleotide capture strands (blue strands). The photocleavable membrane-anchored oligonucleotide capture strands complementary base pair to peptide-DNA conjugates (red strands with blue dots). b) UV irradiation (black lines) induces photocleavage of the *para*-nitrophenyl functional group (yellow star) of the capture strand. c) Duplex DNA-peptide conjugates (red and blue double helix) are then released into solution, leaving the biotinyl-2-nitrosoacetophenone derivative (black star) on the surface. d) The fluid membrane allows for the recovery.

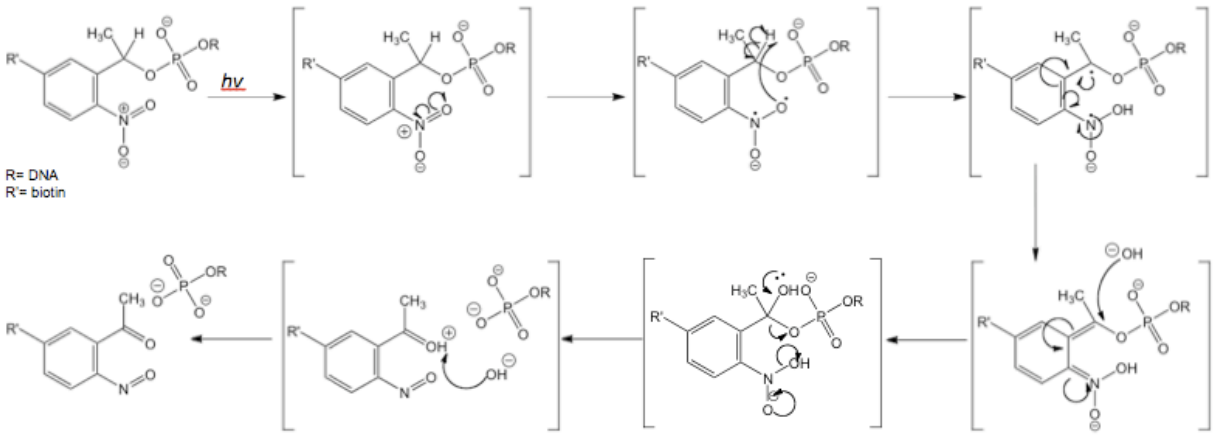

Figure 7: Proposed mechanism for the photocleavage of the nitrobenzyl group after irradiation by UV light based on the photolysis of 2-nitrobenzyl carbonate esters.[21b] Ultraviolet light excites the nitro group, which promotes the formation of radicals. The molecule quenches through rearrangement and subsequent release of the oligonucleotide.

The advantage of this system is three-fold. As the basis for this novel substrate is a supported lipid bilayer, this system is self-healing; it enables reversible recovery of ligand after the photocleavage event. The speed of recovery is dependent on the fluidity of the lipid membrane and can be adjusted by changing the lipid composition. Secondly, this system employs Watson-Crick base-pairing of complementary DNA strands to tether biomolecules into the supported membrane. Due to the specificity of DNA hybridization, multiple ligands can be encoded into the membrane using different pairs of complementary membrane-anchored capture and peptide-conjugated oligonucleotide strands. The light sensitivity is encoded by the presence of the nitrophenyl group. Finally, the photosensitive 5'-modified 2'nitrophenyl functionalization of the membrane-anchored capture strand allows the release of the DNA tethers and ligands into solution to be precisely controlled; the UV irradiation and the resulting photocleavage of the nitrophenyl group can be easily controlled with high spatiotemporal resolution using a standard fluorescence microscope. This self-healing and dynamic light responsive substrate will become a new tool to study integrins and focal adhesions. In

particular, the response of integrin receptors and the cell cytoskeleton to a dynamic signal and released ligand can be probed. Moreover, it can be applied to study other receptor-ligand interactions, as well as endocytosis.

Experimental Methods

Solid-phase synthesis of modified oligonucleotides

Modified oligonucleotides were synthesized using the solid-phase phosphoramidite approach. In particular, the biotinylated capture strands, CC61A, were synthesized using an Expedite 8909 Nucleic Acid Synthesis System (Biolytic Lab Performance, Inc, Fremont, CA), while the complementary strands, CC61A', were purchased from Integrated DNA Technologies (IDT) (Coralville, IA) (Table 1). The phosphoramidite synthetic method to oligonucleotide synthesis is a chemical approach to produce short nucleic acid strands with a defined sequence.[22] Unlike natural biological systems, which use polymerases and templates to synthesize DNA from the 5'-end to 3'-end, this chemical approach does not require templates or primers, and builds the biopolymer from the 3'-end to 5'-end.[22] The typical monomers are 2' deoxynucleosides that are protected with an acid labile dimethoxytrityl group and a phosphoramidite moiety, but a variety of modified monomers are also commercially available (Figure 8). The Expedite 8909 Nucleic Acid Synthesis System is an automated system that cycles through a series of detritylation, coupling, oxidation and coupling steps to produce the desired oligonucleotides.

Table 1: Modified oligonucleotides

Name	Sequence (5' – 3')
CC61A-PC biotin	PC biotin-CCA TAA TTC CAC TAC AAA AAA
CC61A-biotin	Biotin- CCA TAA TTC CAC TAC AAA AAA
CC61A'- Cy3-Am	AmMC6-Cy3-TTT TTT GTA GTG GAA TTA TGG
CC61A'-Am	AmMC6- TTT TTT GTA GTG GAA TT
CC61A'-Acryd	Acryd-TTT TTT GTA GTG GAA TTA TGG

Functionalizations: PC biotin: photocleavable biotin, 1-[2-nitro-5-(6-(N-(4,4'-dimethoxytrityl))

biotinamidocaproamidomethyl)phenyl]-ethyl-[2-cyanoethyl-(N,N-diisopropyl)]-phosphoramidite; Biotin: biotin, 1-dimethoxytrityloxy-2-(N-biotinyl-4-aminobutyl)-propyl-3-O-(2-cyanoethyl)-(N,N-diisopropyl)-phosphoramidite; AmMC6: 5'amino-modifier C6, 6-(4-Monomethoxytritylamino)hexyl-(2-cyanoethyl)-(N,N-diisopropyl)-phosphoramidite, Cy3: Cy3™, 1-[3-(4-monomethoxytrityloxy)propyl]-1'-[3-[(2-cyanoethyl)-(N,N-diisopropyl) phosphoramidityl]propyl]-3,3,3',3'-tetramethylindocarbocyanine chloride; Acryd: 5' acrydite™

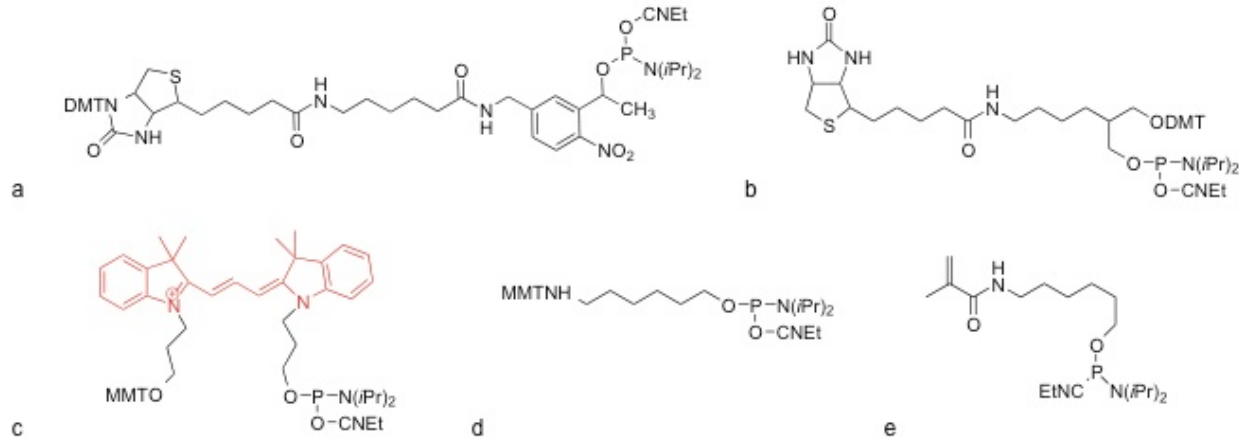

Figure 8: Modified phosphoramidites: a) photocleavable biotin phosphoramidite; b) biotin phosphoramidite; c) Cy 3™ phosphoramidite; d) 5' amino-modifier C6 phosphoramidite; e) acrydite™ phosphoramidite

The four standard DNA monomers, 5' DMT deoxythymidine 3'cyano-ethyl-phosphoramidite (dT CEPA), 5' DMT (N-Bz) deoxyadenosine 3' cyano-ethyl-phosphoramidite (dA (N-Bz) CEPA), 5' deoxy (N-ibu) guanine 3' cyano-ethyl-phosphoramidite (dG (ibu) CEPA), and 5' DMT (N-Bz) deoxycytosine 3' cyano-ethyl-phosphoramidite (dC (N-Bz) CEPA) and the preloaded 1.0 µmole dA (N-Bz), T, dC, and dG (ibu) controlled-pore glass (CPG) columns with a pore size of 1000 Å were purchased from Azco Biotech, Inc. (Oceanside, CA). 1-dimethoxytrityloxy-2-(N-biotinyl-4-aminobutyl)-propyl-3-O-(2-cyanoethyl)-(N,N-diisopropyl)-phosphoramidite or the biotin phosphoramidite, and 1-[2-nitro-5-(6-(N-(4,4'-dimethoxytrityl))-

biotinamidocaproamidomethyl)phenyl]-ethyl-[2-cyanoethyl-(N,N-diisopropyl)]-phosphoramidite or the photocleavable biotin phosphoramidite were purchased from Glen Research (Sterling, VA). The synthesis grade acetonitrile and anhydrous dichloromethane were acquired from Sigma Aldrich Corporation (St. Louis, MA). The mild oxidizer solution of 0.02 M iodine in tetrahydrofuran/pyridine/water (89.6/0.4/10) and the 3% trichloroacetic acid in dichloromethane deblocking solution were acquired from Azco Biotech, Inc. The cap mix A consisting of tetrahydrofuran/ acetic anhydride (9:1), the cap mix B consisting of 10% 1-methylimidazole in tetrahydrofuran/ pyridine (8:1), and the activator solution of 0.45M sublimed tetrazole in acetonitrile were purchased from Glen Research.

Prior to synthesis, 1.0 g of each of the DNA monomers was dissolved in 20 mL of dry acetonitrile and 50 µmoles of the modified bases were dissolved in 0.75 mL of dry acetonitrile, and then placed into the Expedite 8909 Nucleic Acid Synthesis System. The sequence of the desired oligonucleotide and the protocol for the synthesis were created, reviewed and edited using the Expedite Workstation Software. Synthesis of the oligonucleotide occurs under nitrogen gas and begins on the solid support from the 3'end, where the first monomer is attached to a controlled-pore glass (CPG) column. The first step involves removing the trityl protecting group from the 5' carbon of the pentose sugar of the anchored monomer with the deblock solution. This deprotection step is also known as detritylation. Following a wash with acetonitrile, the incoming phosphoramidite is activated using tetrazole, which forms a tetrazole phosphoamidite intermediate that attacks the 5' hydroxyl of the deprotected substrate. This results in a phosphite linkage between the anchored and incoming monomers. The phosphite linkage is then stabilized by oxidation using an iodine solution. In order to prevent reactions to any free 5' hydroxyls remaining, the growing strands are capped irreversibly. The cycle then repeats until the desired sequence is achieved (Figure 9). The protocol was for DMT-ON such that the last base remained protected after synthesis.

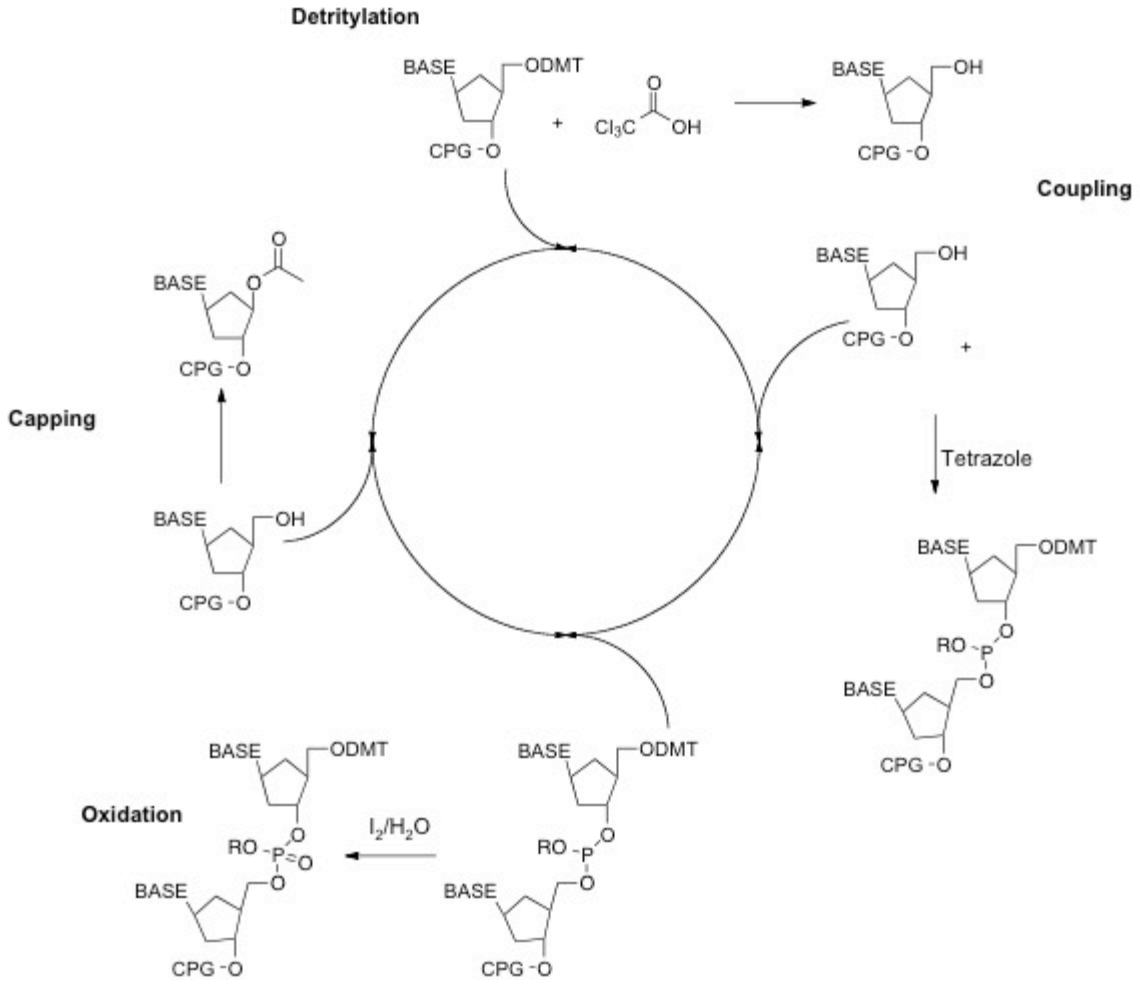

Figure 9: Solid phase oligonucleotide synthesis

Cleavage and deprotection of synthesized oligonucleotides from CPG synthesis columns

The synthesized oligonucleotides were manually cleaved and deprotected from the CPG synthesis column with concentrated ammonium hydroxide and the double syringe method. The puriss. grade ammonium hydroxide (30-33% NH_3 in H_2O) was acquired from Sigma Alrich. An empty disposable 1-mL syringe was loaded onto the synthesis column, while a second syringe filled with 1 mL of fresh ammonium hydroxide was loaded onto the other side. After ensuring the two syringes were fully inserted into the column, the base was carefully injected through the column back and forth three times, and then allowed to stand for 30 minutes. The ammonium

hydroxide was then injected back and forth three times, and allowed to stand for another 30 minutes. Subsequently, the DNA-base solution was drained into a single syringe and stored.

Purification of synthesized oligonucleotides with reverse phase cartridges

The cleaved synthesized oligonucleotides are purified with reverse phase Glen-Pak™ cartridges (Glen Research). These cartridges bind to the 5' DMT protecting group of fully synthesized oligonucleotides. To the 1mL solution of DNA-ammonium hydroxide, 1 mL of a 100 mg/mL sodium chloride solution was added. The disposable syringe version of the cartridges was conditioned by running 0.5 mL of acetonitrile and then 1.0 mL of a 2 M of triethylamine acetate with a flow rate of two drops per second. The DNA/base/salt solution was then injected through the cartridge in 1.0 mL aliquots. Subsequently, two 1.0-mL aliquots of a salt wash solution consisting of 5% acetonitrile in a 100 mg/mL sodium chloride solution and two 1.0-mL aliquots of a 2% trifluoroacetic acid (TFA) solutions were applied to the cartridge. For the synthesized biotinylated oligonucleotides, the TFA solution was left on the cartridge for 10 minutes to allow for complete detritylation of the 5' biotin. The cartridge was then washed with two 1.0-mL aliquots of Milli-Q water. The purified and detritylated synthesized oligonucleotide strands were eluted using 1.0 mL of a 50% acetonitrile in water solution with 0.5% ammonium hydroxide and collected.

Characterization of oligonucleotides

The oligonucleotides were purified and characterized using reverse-phase high-performance liquid chromatography (HPLC) with an Agilent 1100 Series HPLC (Agilent Technologies, Santa Clara, CA). A standard DNA purification protocol was followed for all DNA samples. Buffer A was a 0.1 M solution of triethyl ammonium acetate and buffer B was pure HPLC grade acetonitrile. A gradient of increasing acetonitrile from 8 to 48% over 40 minutes was applied to the sample with a flow rate of 1 mL/min. To characterize the photocleavable CC61A-PC biotin oligonucleotide and its photoreleased form, a dilute sample was irradiated for 10 minutes with a compact 4 watt combination long wavelength and short wavelength UV lamp

(UVP, Upland, CA). A Nanodrop 2000c spectrophotometer was used to determine the absorbance spectrum of the oligonucleotides (Thermo Scientific, Barrington, IL). In particular, the absorbance at 260 nm was used to calculate the concentration of a given oligonucleotide sample using Beer's Law.

Preparation and formation of supported lipid membranes

To generate supported lipid membranes, small unilamellar vesicles with the desire lipid composition were initially prepared.[15a] For the experiments, 2.00 mg/mL lipid solutions consisting of 99.9% bulk unsaturated 1,2-dioleoyl-*sn*-glycero-3-phosphocholine (DOPC) phospholipids (Avanti Polar Lipids, Inc., Alabaster, Alabama) and 0.1% 1,2-dioleoyl-*sn*-glycero-3-phosphoethanolamine-N-(biotinyl) (biotin DPPE) phospholipids (Avanti Polar Lipids, Inc.), phospholipids with the headgroup modified with a biotin moiety, were made (Figure 11). As a control for membrane fluidity, 2.00 mg/mL lipid solutions consisting of 97.90% DOPC, 0.1% of biotin DPPE, and 2% 1-oleoyl-2-(6-((7-nitro-2-1,3-benzoxadiazol-4-yl)amino)hexanoyl)-*sn*-glycero-3-phosphocholine (NBD PC), phospholipid with the fatty acid labeled with a dye (Avanti Polar Lipids), were also used (Figure 10). The lipids were first dissolved and mixed in 3 mL of chloroform. The chloroform was removed using a Rotavapor R-210 rotary evaporator (Buchi, Switzerland), and then with nitrogen gas for 15 minutes. To the dried lipids, 2 mL of ultrapure Milli-Q water was added. The lipid solution was then frozen and thawed three times by swirling in an acetone-dry ice solution and a water bath set to 45˚C, respectively. Subsequently, the lipid solution was extruded 11 times with a LIPEX™ mini-extruder (Northern Lipids Inc., Burnaby, Canada) under high pressure through a 100-nm pore filter.

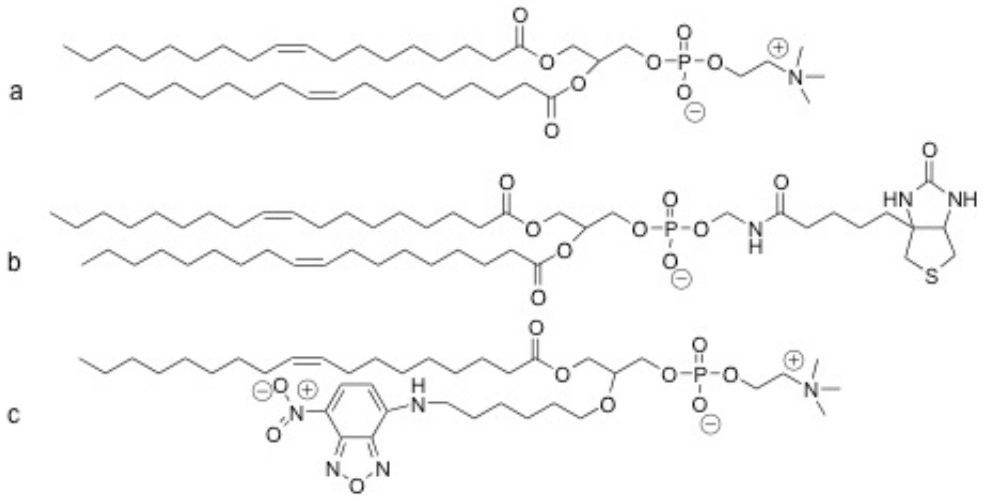

Figure 10: Structure of lipids: a) DOPC; b) biotin PE; c) NBD PC

To form the supported lipid membranes from the prepared small unilamellar vesicles, the wells were first washed with Milli-Q water and then etched with 1 M NaOH for 1 hour. After washing and emptying the wells, 100 µL of solution consisting of 75 µL of a pH 7.4 phosphate buffered saline (PBS) solution, consisting of 0.137 M $NaCl_{(aq)}$, 2.7 mM $KCl_{(aq)}$, 1.4 mM $K_2H_2PO_{4(aq)}$, and 0.01 M $Na_2HPO_{4(aq)}$, and 25 µL of the prepared vesicle solution was added to each well and allowed to incubate for 20 minutes. The small unilamellar vesicles self-assemble into planar lipid bilayers. After incubation, the wells were rinsed three times with 5 mL of water and then twice with 5 mL of PBS.

Functionalization of supported lipid membrane with hybridized DNA

Prior to adding streptavidin to the supported lipid bilayers, the lipid bilayers were blocked for 30 minutes with 200 µL of a solution consisting of 40 µL of a 1 mg/mL of bovine albumin serum solution and 160 µL of PBS. After rinsing the BSA, a total of 0.8 µg of streptavidin in a 200 µL solution of PBS was added to each well. While the streptavidin incubated on the surface of 45 minutes, 50 µL of a 0.342 µM CC61A- PC biotin solution and 50 µL of a 0.335 µM CC61A-biotin solution were each allowed to hybridize to a 50 µL of a 1.00 µM CC61A'-Cy3- Am solution. The complementary oligonucleotides were heated to 50 ˚C for 10 minutes and allowed

to cool back down to room temperature. The surfaces were rinsed of the streptavidin and 100 µL of the hybridized DNA solutions were added and allowed to incubate for 45 minutes.

Characterization of the membrane-anchored DNA strands

The DNA functionalized surfaces were visualized using fluorescent microscopy with a Nikon Ti Eclipse microscope(Nikon, Japan), featuring Evolve EM CCD (Photometrics), an Intensilight epifluorescence source (Nikon), and a total internal reflection fluorescence (TIRF) launcher with two laser lines: 488 nm (10 mW) and 647 nm (20 mW). Chroma filter cubes were used for the experiments. Fluorescence recovery after photobleaching (FRAP) was used to determine the fluidity of the supported lipid bilayers. To observe the NBD lipids as a control for the surface fluidity, the surfaces were photobleached with the FITC filter cube (535-550 nm), then immediately imaged using the TIRF 488 filter cube (525-550 nm) and then once more after 30 seconds. For the Cy3-labeled duplex DNA functionalized surfaces, the DAPI filter cube (325- 375nm) was used to irradiate the DNA for 15 seconds, while the TRITC filter cube (620-660 nm) was used to observe the Cy3 label. To determine the kinetics of photorelease of duplex, the photocleavable surface's exposure to UV light as a function of time was varied. After UV irradiation, the surface was imaged immediately with a 300 ms exposure to the TRITC cube. The 10 UV exposure time durations included 300 ms, 700 ms, 1 s, 2 s, 3 s, 5 s, 8 s, 12 s, 20 s, and 60 s.

Conjugation of cRGD peptide to single-stranded oligonucleotide

To conjugate a minimum cell adhesive cyclic RGD peptide, we chose to use the heterobifunctional linker, 4-(9N-maleimidomethyl)cyclohexane-1-carboxylic acid 3-sulfo-N-hydroxysuccinimide ester sodium (sulfo-SMCC).[23] The *N*-hydroxysuccinimide ester (NHS ester) at one end reacts with primary amines to form stable amide bonds, while the maleimide at the other end reacts with sulfhydryl groups to produce thioester bonds. The selectivity of the amine for the NHS ester and the sulfhydryl for the maleimide can be controlled using pH.[23b] This linking system had been used previously for enzyme-antibody[24], antibody- oligonucleotide[25], and

fluorescent protein-oligonucleotide conjugates[26]. For the cRGD-oligonucleotide conjugate needed for this experimental platform, the oligonucleotide was amine-modified, while the cRGD had a reactive cysteine.

Optimization of the NHS ester-amine coupling first cRGD-oligonucleotide conjugation

In order for the conjugation of the oligonucleotide to the cRGD peptide to occur, both the NHS ester-amine coupling and the maleimide-thiol coupling must occur. To minimize the effects of the competing hydrolysis of the NHS ester, the reaction between the amine-modified DNA and the sulfo-SMCC was allowed to proceed first.

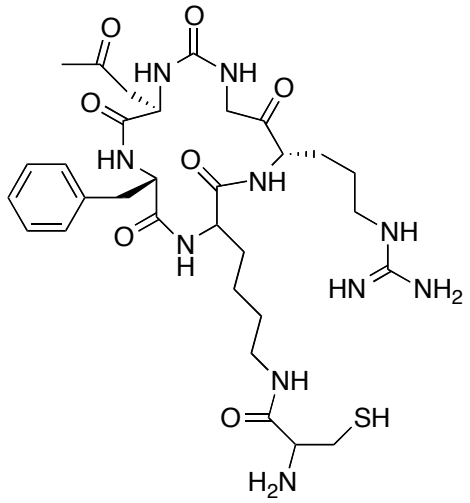

Figure 11: Structure of cRGD-SH-NH_2

A non-complementary test 3'-amine modified oligonucleotide, YN052810A, was used to optimize the reactions. 6.0 µL of a 0.74 mM solution of YN052810A oligonucleotide was added to a 32.0 µL of pH 8.0 100 mM KH_2PO_4 buffer. 2 µL of 0.08 M sulfo-SMCC in dimethyl sulfoxide (DMSO) solution was added to the mixture and allowed to react for 1.5 hours at room temperature.

The oligonucleotide was isolated from excess sulfo-SMCC by ethanol purification. 5 µL of 3 M sodium acetate and 100 µL of cold ethanol were added to the sample. The sample was subsequently stored in the -20 ˚C freezer for 30 minutes and then centrifuged for 5 minutes. The supernatant was discarded and the pellet was mixed with another 100 µL aliquot of cold ethanol. After 30 minutes in the -20 ˚C freezer, the sample was centrifuged and the supernatant was discarded. The oligonucleotide pellet was dried using a SC110A SpeedVac® Plus (Thermo Savant).

The purified oligonucleotide was resuspended in 148 µL of pH 7.5 100 mM KH_2PO_4 buffer. 3.14 µL of 1 mg/mL of *cyclo*(Cys-Arg-Gly-Asp-*D*-Phe-Lys-(Cys)) (cRGD-SH-NH_2) (Peptides International, Louisville, KY in PBS buffer (pH 7) was added to the oligonucletide solution (Figure 11). In order to aid in the identification of the absorbance peaks, 0.417 µL of 0.05 M of 5-(and 6-) carboxyfluorescein succinimydyl ester, NHS-fluorescein (Thermo Scientific), in DMSO was added to the reaction mixture. The NHS-fluorescein can react with the reactive amine of cRGD-SH-NH_2 and label the peptide (Figure 12). The reaction was allowed to proceed over night at room temperature (Figure 13).

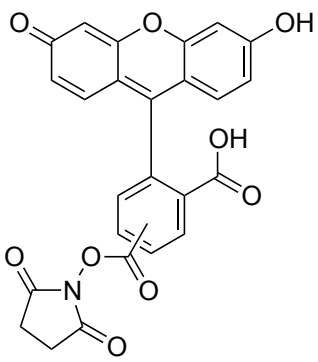

Figure 12: Structure of NHS-fluorescein

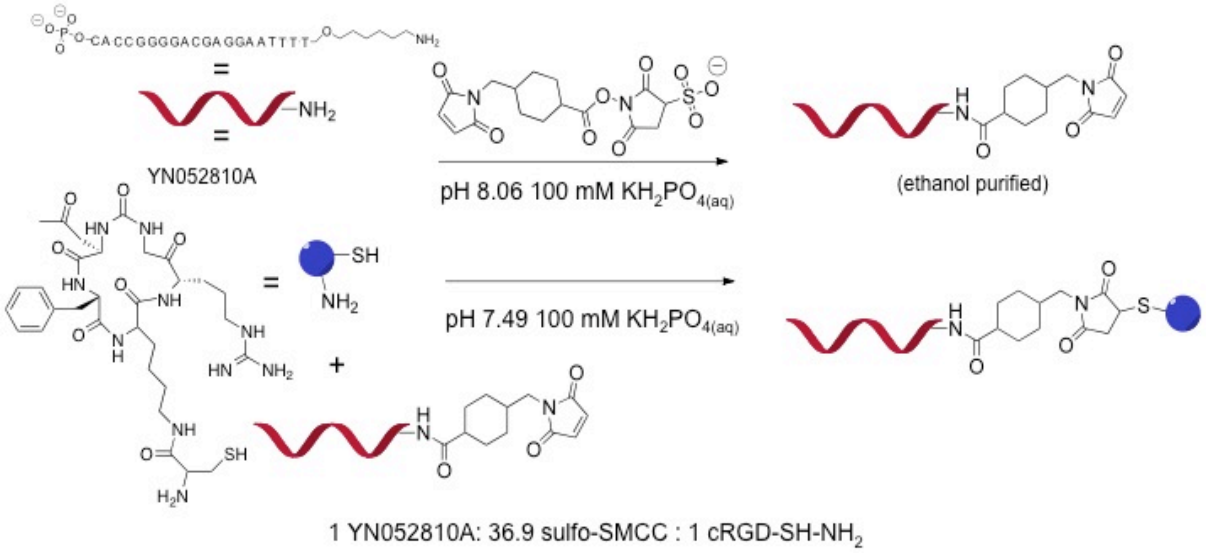

Figure 13: Reaction scheme for NHS ester-amine coupling first cRGD-oligonucleotide conjugation

The reaction products were characterized using reverse-phase HPLC, following standard oligonucleotide purification protocol. The NHS-fluorescein label was observed using

the 494 nm absorbance. To aid in the identification of the absorbance peaks, oligonucleotide-SMCC, cRGD-SH-NH_2, dye-labeled cRGD-SH-NH_2, and free dye were characterized with the same HPLC method.

Reduction of disulfides with immobilized TCEP disulfide reducing gel

To generate free thiols from disulfide bonds formed between cRGD peptides, immobilized tris(2-carboxyethyl) phosphine hydrochloride (TCEP) disulfide reducing gel (Thermo Scientific, Barrington, IL) was used. The volume of the TCEP reducing gel slurry used was dependent on the volume of peptide solution; in general, a volume 5 µL greater than the peptide volume was used. The TCEP slurry was washed with the pH 7.5 100 mM KH_2PO_4 solution three times by centrifuging the slurry, removing the supernatant and adding the buffer. After discarding the supernatant of the final wash, the 1 mg/mL peptide solution was added. The TCEP and peptide solution were allowed to incubate for 50 minutes. The mixture was occasionally vortexed to resuspend the gel into the peptide solution. After incubation, the mixture was centrifuged and the peptide-containing supernatant was collected. For coupling procedures, the reduced peptide solution was added immediately to the DNA-SMCC solution.

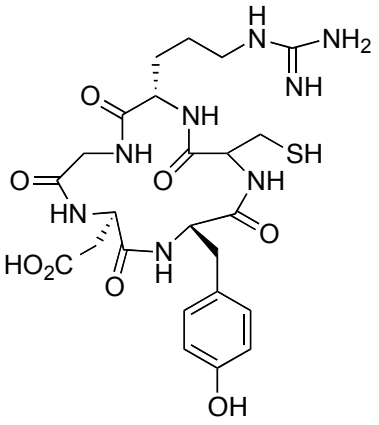

Figure 14: Structure of cRGD-SH

Characterization of cyclo(Arg-Gly-Asp-D-Try-Cys)

In order to optimize reaction conditions for the maleimide and thiol coupling and identify peaks in reverse phase HPLC spectra, a cRGD that had a reactive thiol, but lacked an amine, was acquired from Peptides International (Louisville, KY) (Figure 14). 1mg of *cyclo*(Arg-Gly-Asp-*D*-Try-Cys) (cRGD-SH) was dissolved in 50 µL of 3% acetic acid and 950 µL of Milli-Q water for a concentration of 1 mg/mL or 1.68 mM. A sample of the peptide was run on reverse phase HPLC to determine absorbance peaks at 220 nm, following the protocol for oligonucleotide

characterization. A sample of the peptide after being treated with the TCEP reducing gel slurry was also characterized by reverse phase HPLC.

The cRGD-SH peptide was directly coupled to the sulfo-SMCC. 25 µL of the 1 mg/mL peptide solution after treating with TCEP reducing gel slurry in the pH 7.5 100 mM KH_2PO_4 solution and 1 µL of a 0.8 M sulfo-SMCC in DMSO solution were mixed and allowed to react at room temperature overnight. The products were characterized using reverse phase HPLC using the standard DNA purification protocol.

Optimization of the maleimide-thiol coupling first cRGD-oligonucleotide conjugation

Although the NHS ester-amine DNA-sulfo-SMCC coupling and maleimide-thiol peptide-sulfo-SMCC coupling were successful separately and could be observed through reverse phase HPLC, we were unable to perform both reactions in series and produce a cRGD-oligonucleotide conjugate. As a result, we chose to run the reactions in reverse order and allow the sulfo-SMCC couple to the cRGD peptide before introducing the amine-functionalized oligonucleotide. In order to optimize the reaction conditions for cRGD-oligonucleotide conjugation in which the maleimide of the sulfo-SMCC and the cysteine of the cRGD peptide were allowed to react first, six reaction mixtures were run simultaneously (Figure 15). Two variables, the buffer and the length of time for the first coupling, were of interest due to the potential of hydrolyzing the NHS ester.

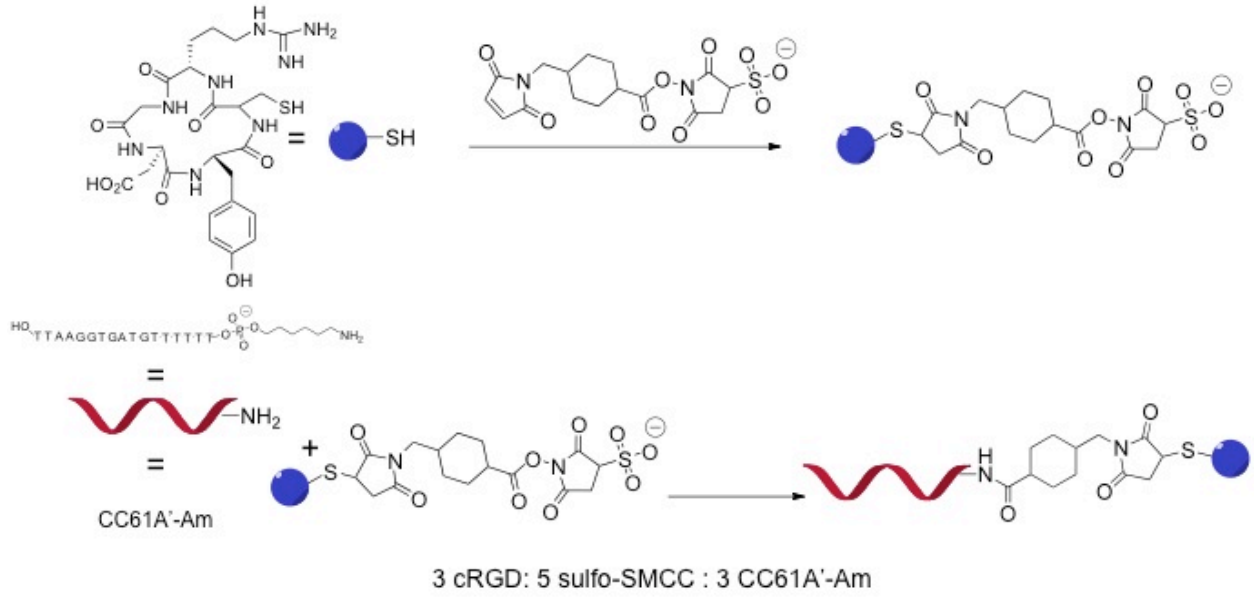

Figure 15: Reaction scheme for maleimide-thiol coupling first cRGD-oligonucleotide conjugation

For each of the six reaction mixtures, 17.8 µL of the 1 mg/mL cRGD-SH solution was mixed with 20 µL of one of three solvents: a buffer of pH 7 100 mM KH_2PO_4 solution, DMSO, or dimethylformamide (DMF). 1.1 µL of a 0.05 M sulfo-SMCC in DMSO solution was added to each mixture. Before the amine-modified oligonucleotide, CC61A'-Am, was introduced, one half of the reaction mixtures, of which all buffers were represented, was allowed to react for 1.5 hours, while the other half was allowed to react for 3 hours. Upon addition of 32.7 µL of 0.9 mM CC61A'-Am, 2 µL of 1 M NaOH and 20 µL of pH 8.0 100 mM KH_2PO_4 solution were also mixed to the raise the pH of the reaction mixture. The coupling reaction was allowed to run overnight at room temperature. The products were characterized using reverse phase HPLC and the largest peak, with retentions times ranging from 10 minutes to 11.5 minutes, for each of the reaction mixtures that coupled for 3 hours was collected and dried. The absorbance spectrum of the collected products was determined using the Nanodrop.

Characterization of the interactions between cells and membrane-anchored DNA, cRGD and potential cRGD-oligonucleotides

The supported lipid membranes consisting of 0.1% biotin DPPE and 99.9% DOPC were prepared and blocked with BSA. To each well, 0.8 µg of streptavidin was added and allowed to incubate for 45 minutes. For the negative control, the surface would be functionalized with duplex CC61A-biotin/CC61A'-Cy3-Am DNA and unlabelled streptavidin was used. For the potential cRGD-oligonucleotide, and the positive control, biotinylated RGD, streptavidin labeled with the fluorophore Alexa 647 was used. The product collected at 10.86 minutes of the HPLC run for the reaction mixture with DMF served as the potential cRGD-oligonucleotide; 0.5 µL of the product was diluted into 95.5 µL of PBS. The CC61A-biotin oligonucleotide was allowed to hybridized to each of CC61A'-Cy3-Am and the potential cRGD-oligonucleotide. Once the surfaces were rinsed of the streptavidin, 100 µL of the hybridized DNA solutions were added to their corresponding surfaces and allowed to incubate for 40 minutes. For the positive control, 8 µL of 1 µM solution of biotinylated cRGD was diluted to 25 µL with PBS, added to the surfaces and allowed to incubate.

In order to obtain direct evidence of a cRGD-oligonucleotide conjuate, we sought to observe cell adhesion using the HCC1143 breast cancer cell line. Integrin-expressing HCC1143 breast cancer cell line was released from the cell culture flask using 0.05% trypsin. Warm cell imaging media (Hank's buffered salts and HEPES) was transferred into the experimental wells. The cells were counted using a hemacytometer and plated 25,000 cells onto each surface. The 96 well plate was incubated at 37 ˚C and 5% CO_2 for 30 minutes and then imaged on the fluorescence microscope. The 100x objective was warmed to 37 ˚C. The surfaces and the cells were imaged using bright-field, reflection inference constrast microscopy (RICM), TRIC filter cube and the TIRF 640 channel.

Results and Discussion

Characterization of synthesized oligonucleotides

The single-stranded oligonucleotides, CC61A-PC biotin, CC61A-biotin and CC61A'-Cy3, were first characterized using reverse-phase HPLC. For the CC61A-PC biotin oligonucleotide, dilute samples before and after UV irradiation with a standard UV lamp were characterized for absorbance at 260 nm (Figure 16). Prior to photocleavage, the light sensitive oligonucleotide had peaks at 15.1 and 15.3 minutes. The double peaks arise from the resonance structures of the *para*-nitrophenyl group. However, after irradiation, there was a marked shift in retention time to 12 minutes, resulting from the loss of the hydrophobic acyl linker and the biotinyl-2-nitrosoacetophenone derivative. The CC61A-biotin oligonucleotide had a strong peak at 13.4 minutes; the less hydrophobic biotin functionalization group compared to the photocleavable biotin group resulted in a shorted retention time (Figure 17). The dye-labeled complement, CC61A'-Cy3-Am, was characterized for its absorbance at 260 nm, the absorbance of DNA, and at 550 nm, the maximum excitation wavelength for Cy3 (Figure 18). Both the 260 nm and 550 nm peaks coincided at a retention time of 23.0 minutes, showing that the oligonucleotide was properly labeled with the dye.

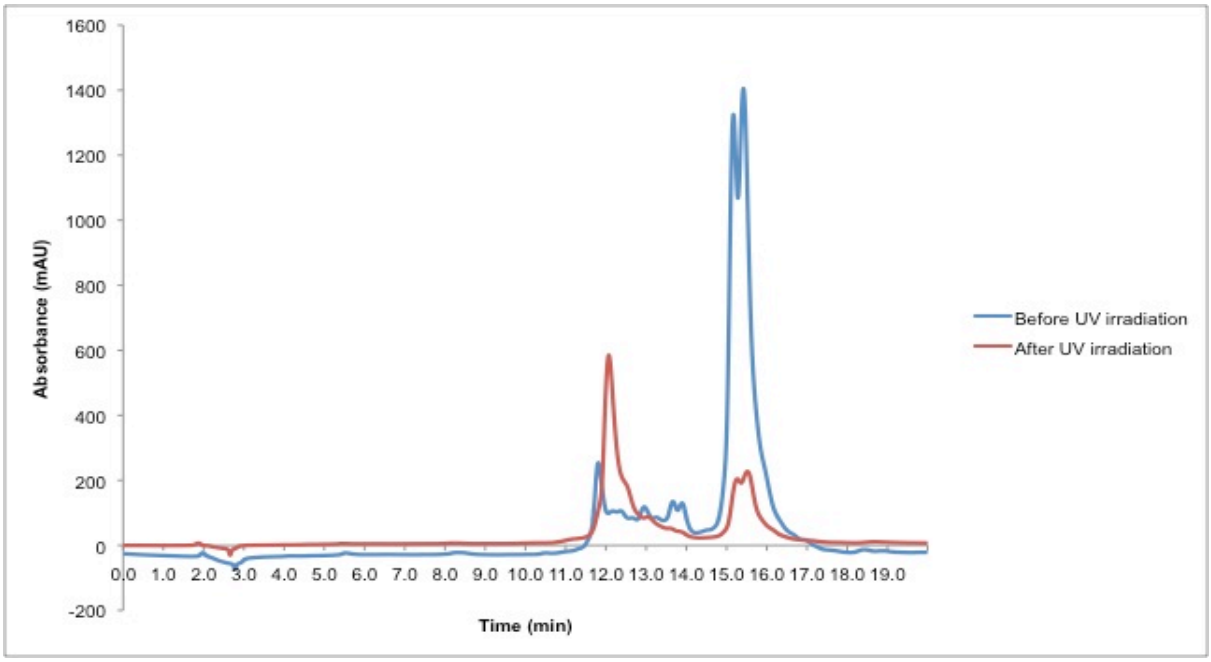

Figure 16: Characterization of photocleavable CC61A-PC biotin single-stranded DNA using HPLC for the absorbance of DNA at 260 nm. Irradiation of a solution of photocleavable DNA with a standard UV lamp for 10 minutes resulted in a marked difference in retention time between the DNA and its photoreleased form.

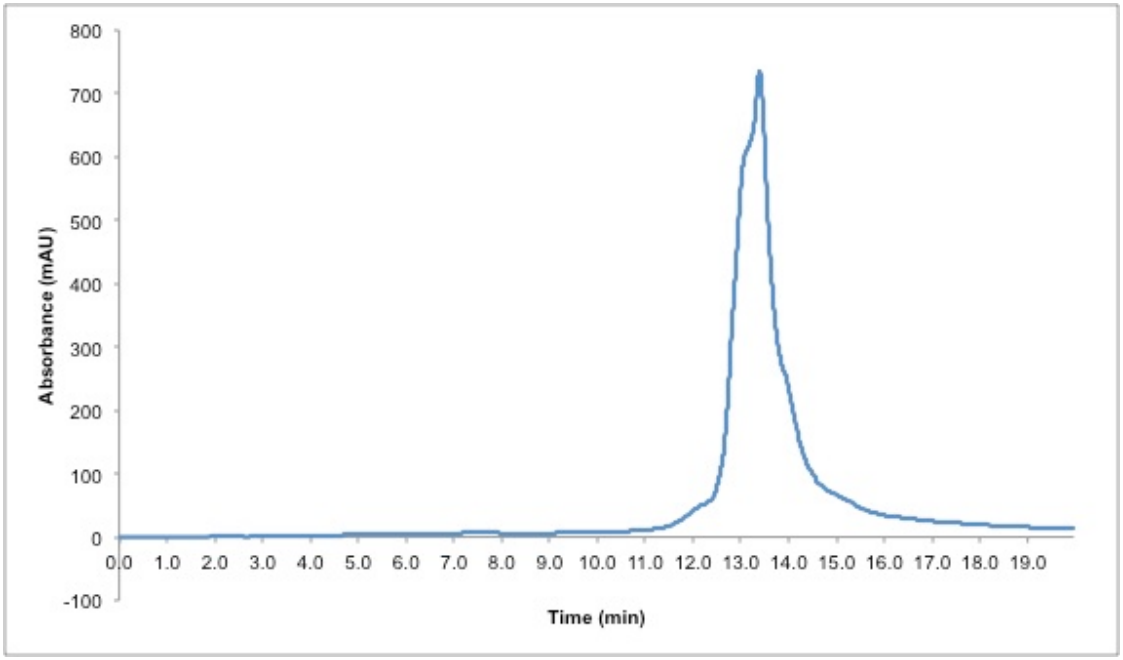

Figure 17: Characterization of CC61A-biotin single-stranded DNA using HPLC for the absorbance of DNA at 260 nm.

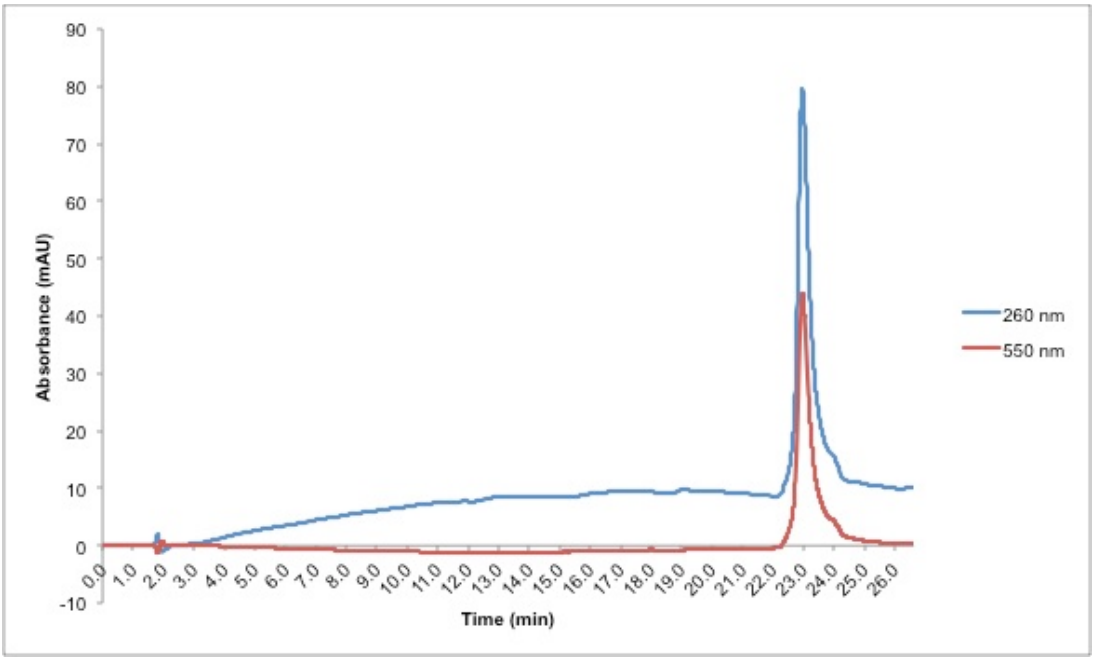

Figure 18: Characterization of dye-labeled CC61A'- Cy3-Am single-stranded DNA using HPLC for the absorbance of DNA at 260 nm and at 550 nm. The coinciding peaks show that the DNA was labeled with the Cy3 dye.

Characterization of the membrane-anchored DNA strands

The fluidity of the supported lipid membranes was qualitatively determined by observing a control surface consisting of 2% NBD lipids. The control surface was photobleached with the FITC filter cube and then allowed to recover. Images taken immediately after photobleaching and after 30 seconds of recovery with the TIRF 488 channel showed the gradual loss of a dark area, as new fluorophores diffused into the photobleached area, indicating that the membrane was fluid (Figure 19).

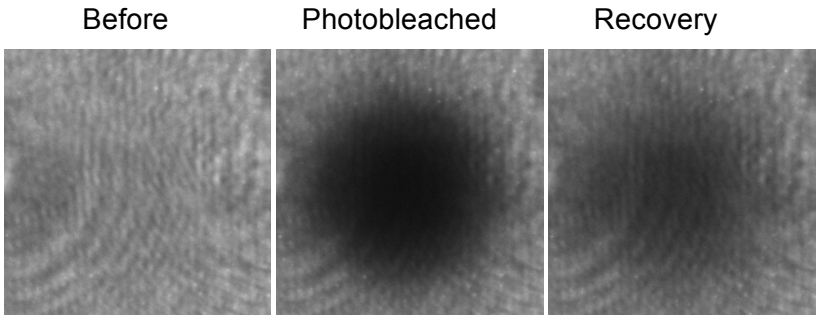

Figure 19: Fluorescence recovery after photobleaching (FRAP) of the control surfaces consisting on of NBD lipids demonstrate membrane fluidity.

The two biotinylated capture strands, CC61A-PC biotin and CC61A-biotin, were both fully complementary to the CC61A'-Cy3-Am dye-labeled strand, but differed by the presence of the photocleavable *para*-nitrophenyl group. Visualization of the surfaces with either of the one of capture strands with the TRITC channel demonstrated that the duplex DNA was incorporated into the lipid membrane. The DAPI filter cube (325nm- 375nm) was used to irradiate both types of the tethered Cy3-labelled duplex DNA of surfaces. However, a decrease in Cy3 fluorescence was only apparent for duplex DNA with the CC61A-PC biotin capture strands (Figure 20, 21, 22). This showed that the loss of fluorescence was due to the release of DNA from the surface, resulting from the photocleavage event, rather than photobleaching of the Cy3 dye with UV light. Fluorescence recovery of the CC61A-PC biotin membranes resulted from the diffusion of new DNA into the irradiated area. The difference in initial fluorescence intensities between the two types of surfaces may be the result of the linker length differences; the photocleavable biotin phosphoramidite has a longer linker than the biotin phosphoramidite and thus the dye was further away from the surface for the CC61A-PC biotin surfaces.

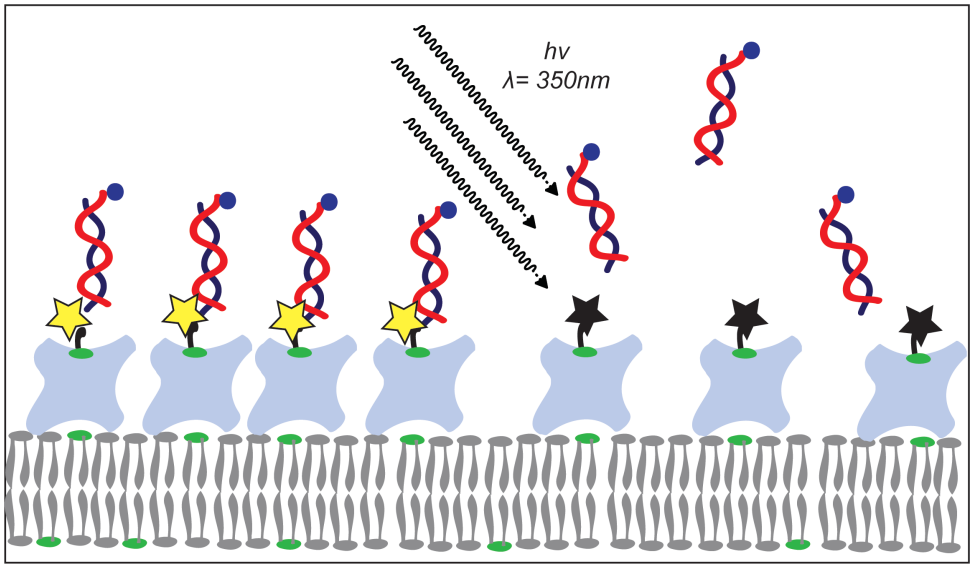

Figure 20: Schematic of the photorelease of duplex DNA from the supported lipid membrane. The DNA (the red and blue double helix) is anchored to the surface using a biotin-streptavidin chemistry. (The green dot and the light blue block represent biotin and streptavidin, respectively) Upon photocleavege, the DNA is released into solution, leaving the biotinyl-2-nitrosoacetophenone derivative (the black star) on the surface.

a. 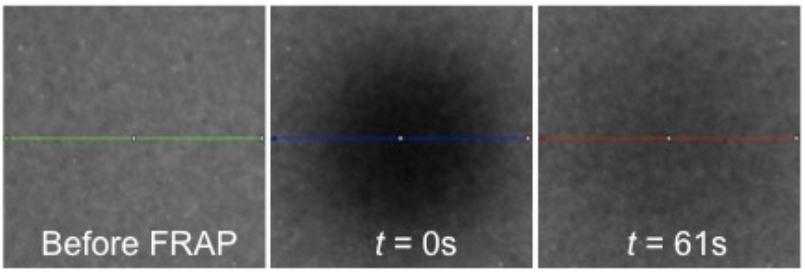

b.

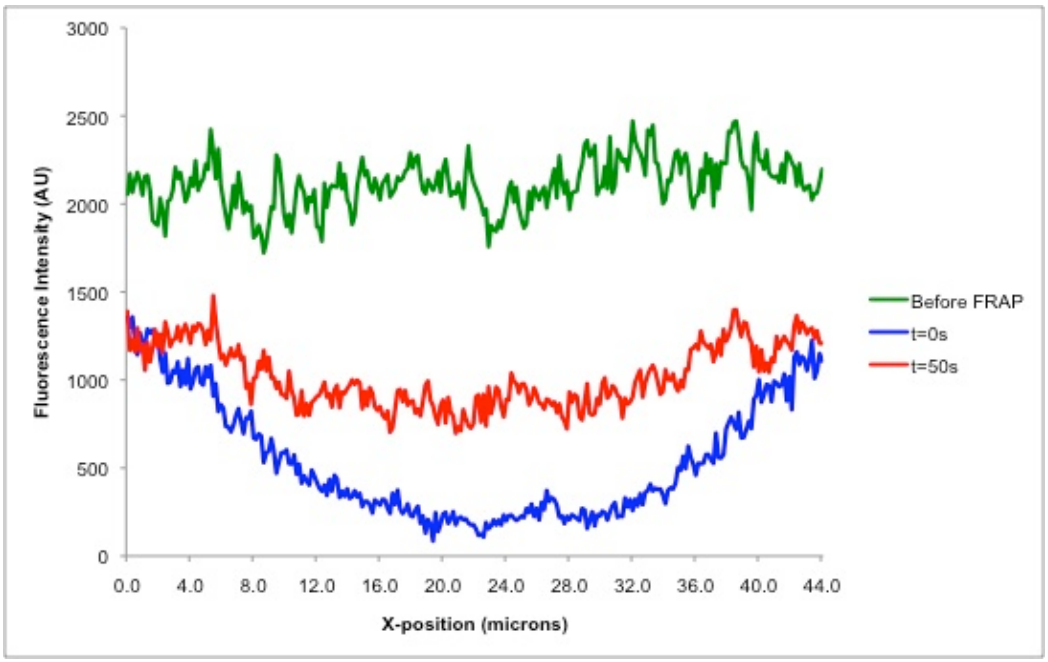

Figure 21: a) Images of CC61A-PC biotin/CC61A'-Cy3-Am duplex DNA functionalized supported lipid bilayer and b) the associated line scan. After 15 seconds of UV irradiation, the CC61A-PC biotin surface showed a marked decrease in Cy3 fluorescence. After 61 seconds, there was some recovery of the loss fluorescence.

a.

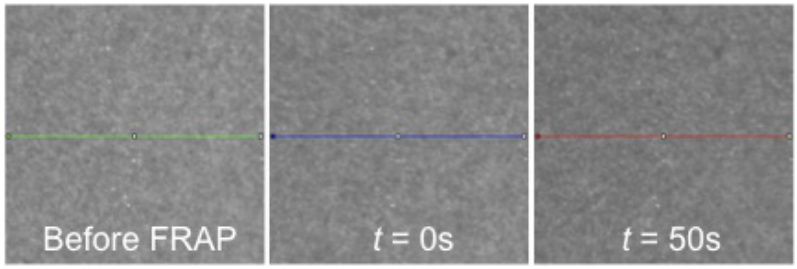

b. 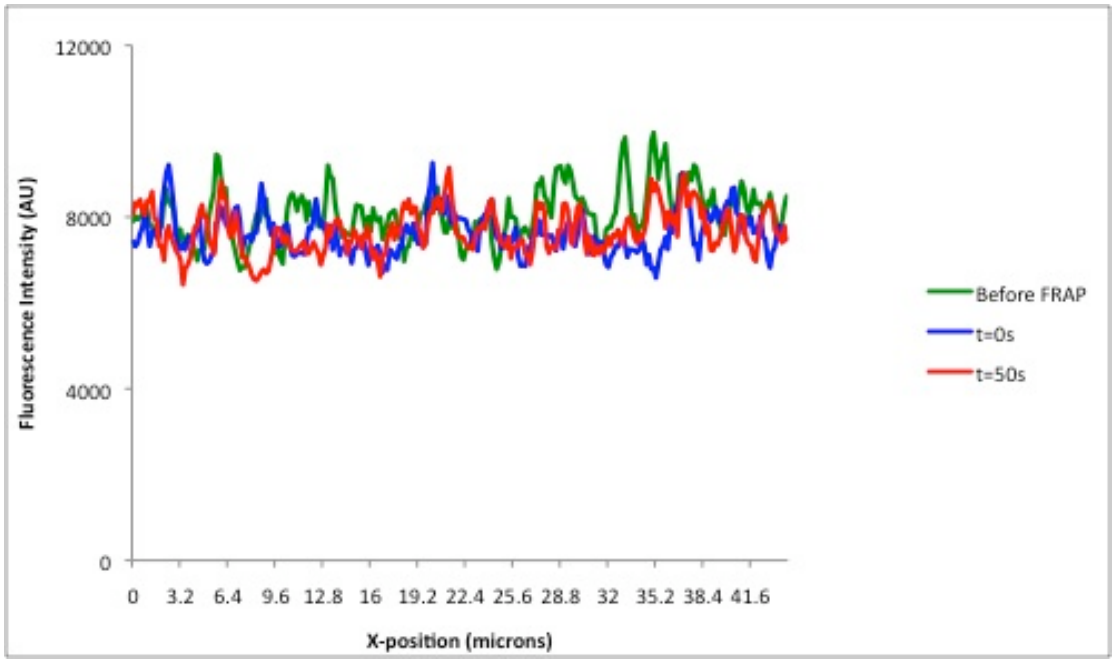

Figure 22: a) Images of CC61A-biotin/CC61A'-Cy3-Am duplex DNA functionalized supported lipid bilayer and b) the associated line scan. After 15 seconds of UV irradiation, the CC61A-biotin surface did not have any apparent loss of fluorescence. After 50 seconds, the fluorescence intensity remained constant.

To determine the kinetics of DNA photorelease, the photocleavable surface's exposure to UV light as a function of time was varied; ten exposure durations, 300 ms, 700 ms, 1 s, 2 s, 3 s, 5 s, 8 s, 12 s, 20 s, and 60 s, were investigated. To normalize the loss of fluorescence intensity, the average intensity of an irradiated area immediately after exposure was compared to the same area before exposure. The intensity of the fluorescence decreased as the length of the UV light increased (Figure 23). The decay can be described with a τ^{-1} of 0.115; only one-third of the original fluorescence remained after 11.6 seconds.

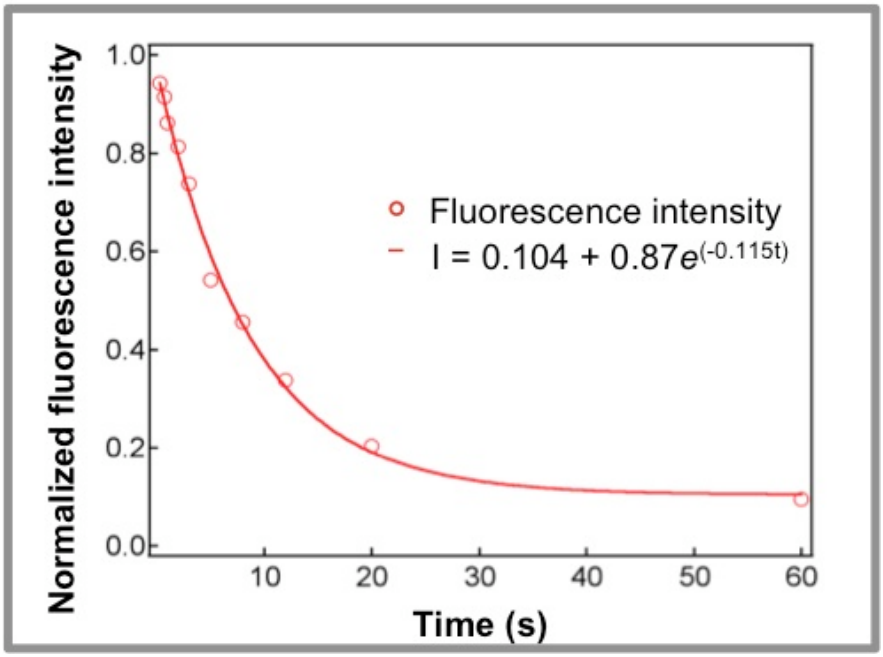

Figure 23: Kinetics of photorelease determined from ten UV light exposure times

Characterization of the NHS ester-amine coupling first cRGD-oligonucleotide conjugation

The products of the NHS ester-amine coupling first cRGD-oligonucleotide conjugation were characterized by reverse phase HPLC. Although, the fluorescein-labeled peaks were clearly visualized with the HPLC, no desired dye-labeled cRGD-oligonucleotide conjugate was present.

Consequently, the individual coupling reactions were investigated. The model amine-modified oligonucleotide, YN052810A, was allowed to react with sulfo-SMCC, and a peptide was not introduced. The products of the reaction mixture were characterized using reverse phase HPLC (Figure 24). There was a shift in the retention time of the main oligonucleotide peak for the absorbance at 260 nm from 10.3 minutes to 13.3 minutes, indicating that the NHS ester of the sulfo-SMCC reacted with the oligonucleotide, thereby making it more hydrophobic.

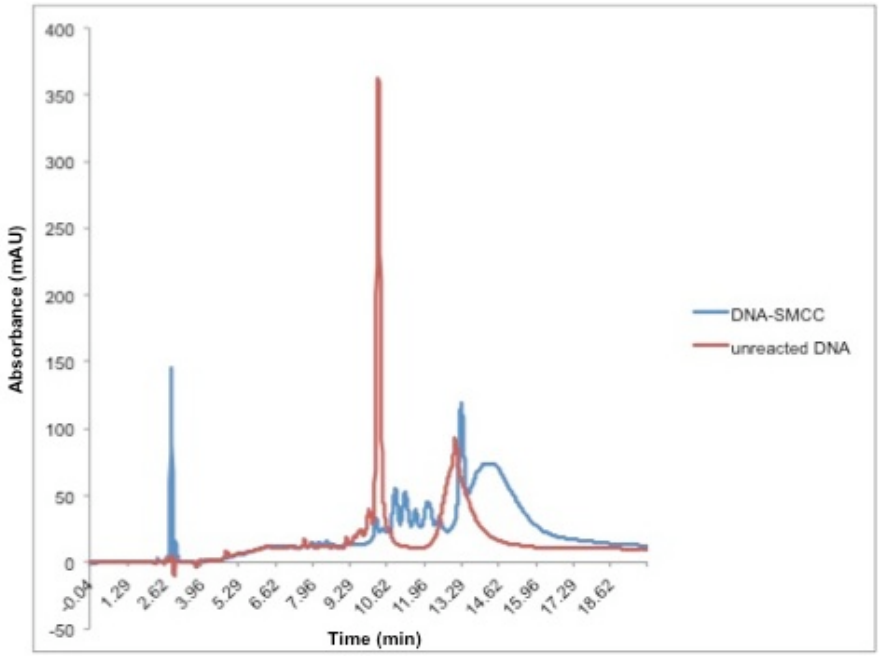

Figure 24: Characterization of YN052810A oligonucleotide before and after reaction with SMCC using HPLC for the absorbance at 260 nm.

Characterization of cRGD-SH

A cyclic RGD peptide that had a reactive thiol, but lacked an amine, *cyclo*(Arg-Gly-Asp-*D*-Try-Cys) (cRGD-SH) was characterized using reverse phase HPLC for absorbance at 220 nm with the standard DNA purification protocol (Figure 25). Due to the possibility of disulfide bond formation between peptides, the cRGD-SH was also characterized using HPLC for absorbance at 220 nm after treatment with the TCEP reducing gel. The lost of the cRGD-SH peak at 11.9 minutes after TCEP treatment indicated that the free thiol form of the peptide had a retention time at 9.11 minutes and was the predominant form of the peptide; the minor peak at 11.9 minutes was the disulfide form.

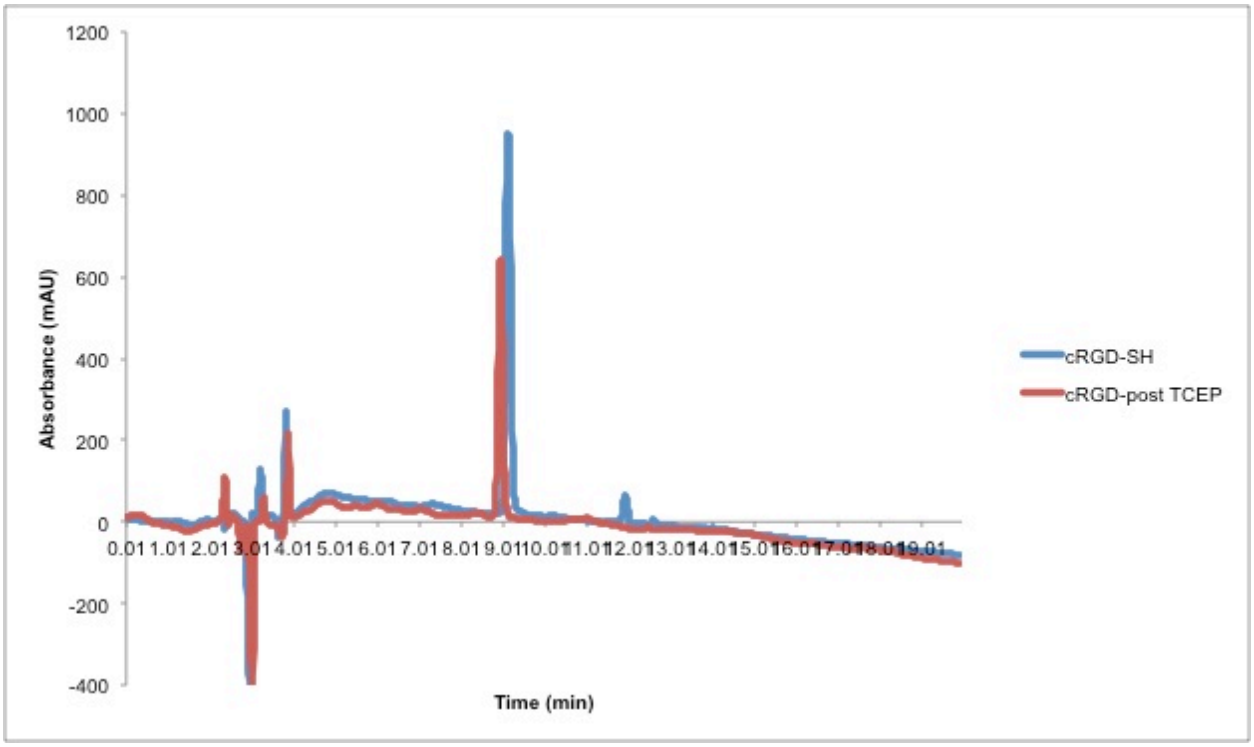

Figure 25: Characterization of cRGD-SH before and after treating with TCEP reducing gel using HPLC for the absorbance at 220 nm.

The cRGD-SH was allowed to directly couple to sulfo-SMCC. The products of the reaction mixture were characterized with HPLC for the absorbance at 220 nm (Figure 26). The lost of the peaks at 9.11 minutes and 11.9 minutes, which corresponded to free peptide, indicated that the reaction proceeded to completion. New peaks arose from the cRGD-SMCC conjugate as well as excess sulfo-SMCC and products of NHS ester hydrolysis.

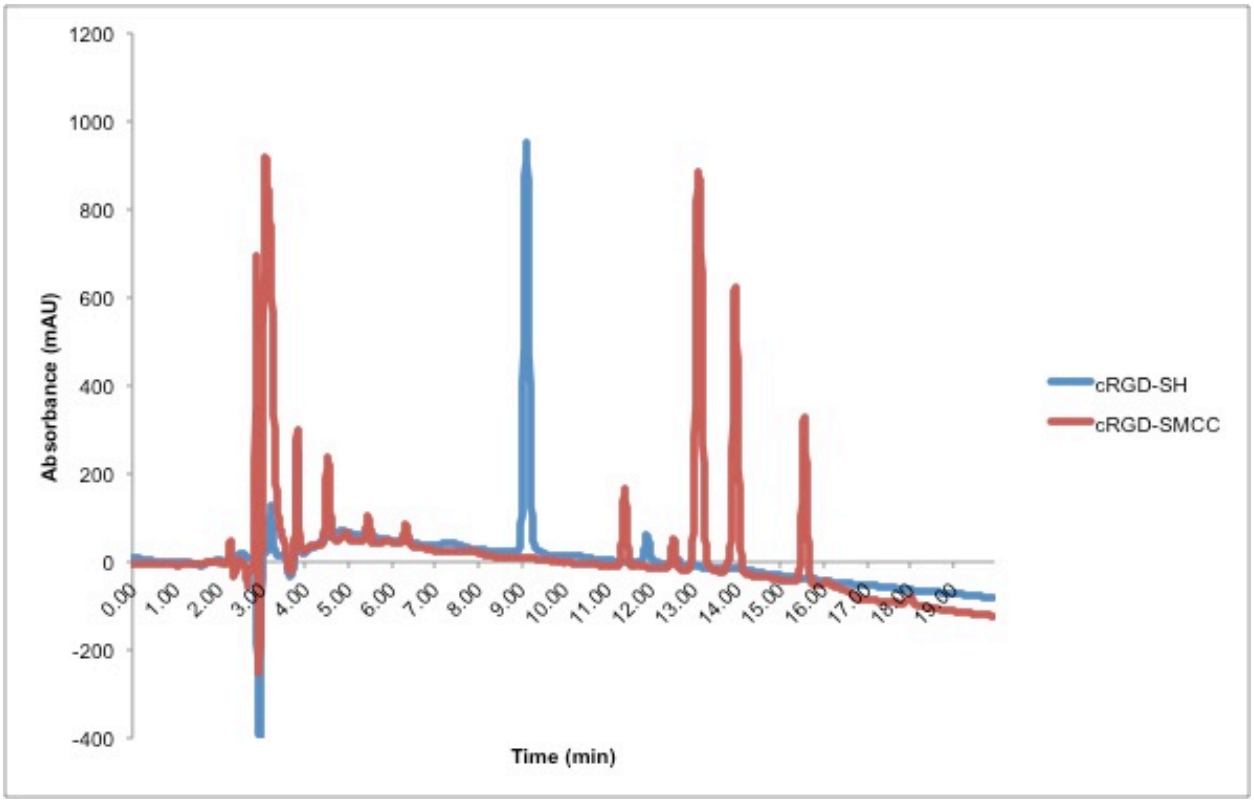

Figure 26: Characterization of products of cRGD and sulfo-SMCC conjugation using HPLC for the absorbance at 220 nm

Characterization of the maleimide-thiol coupling first cRGD-oligonucleotide conjugation

In order to optimize the conditions to couple cRGD to CC61A'-Am DNA, six reactions were allowed to occur simultaneously with different buffers and maleimide-thiol coupling times. The products of the six reactions were characterized using reverse-phase HPLC using the standard oligonucleotide purification method (Figure 27). The absorbance at 260 nm, 280 nm and 220 nm of the strongest peak were compared to the peak for the unreacted CC61A'-Am oligonucleotide, which had a retention time of 10.85 minutes (Figure 28). Although the retention time of the peaks did not greatly differ between the unreacted oligonucleotide and the products of the six reaction mixtures, the ratios comparing the areas for the 280 nm and 260 nm absorbance, and the areas for the 220 nm and 260 nm absorbance were dramatically different

(Table 2).

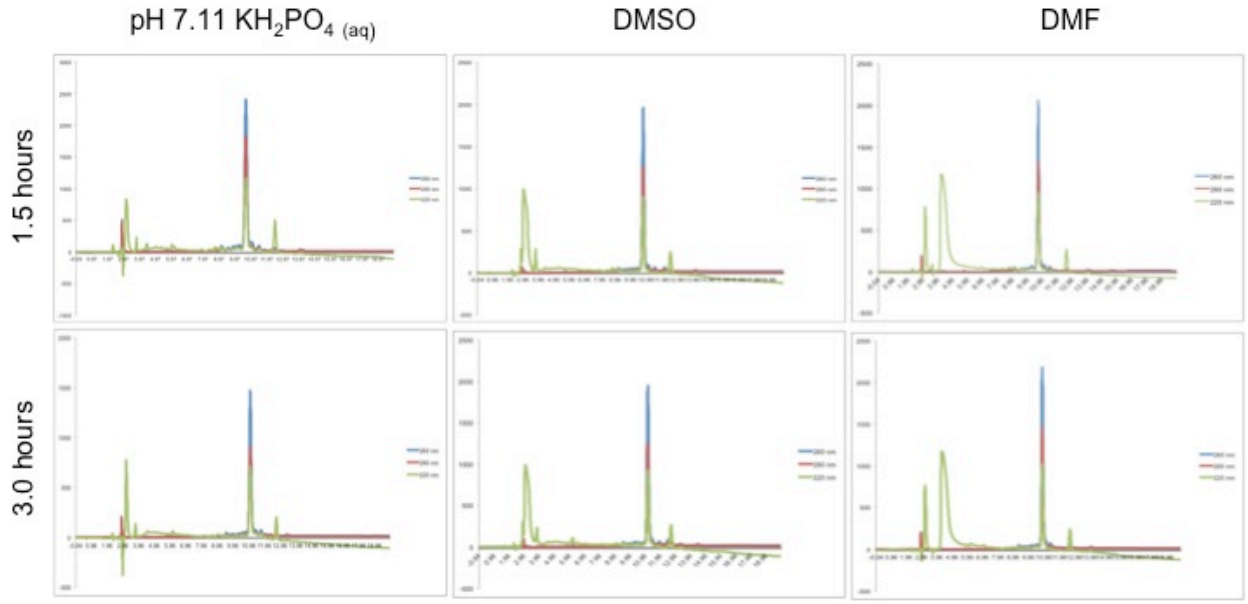

Figure 27: Characterization of the products of the maleimide-thiol coupling first cRGD-oligonucleotide conjugation reactions using reverse-phase HPLC. Six different reaction conditions were used in order to optimize the conjugation. The buffer solutions were pH 7.11 100 mM $KH_2PO_{4(aq)}$, DMSO, and DMF, while the maleimide coupling times were 1.5 hours and 3.0 hours. Absorbance at 260 nm (blue), 280 nm (red) and 220 nm (green) were monitored.

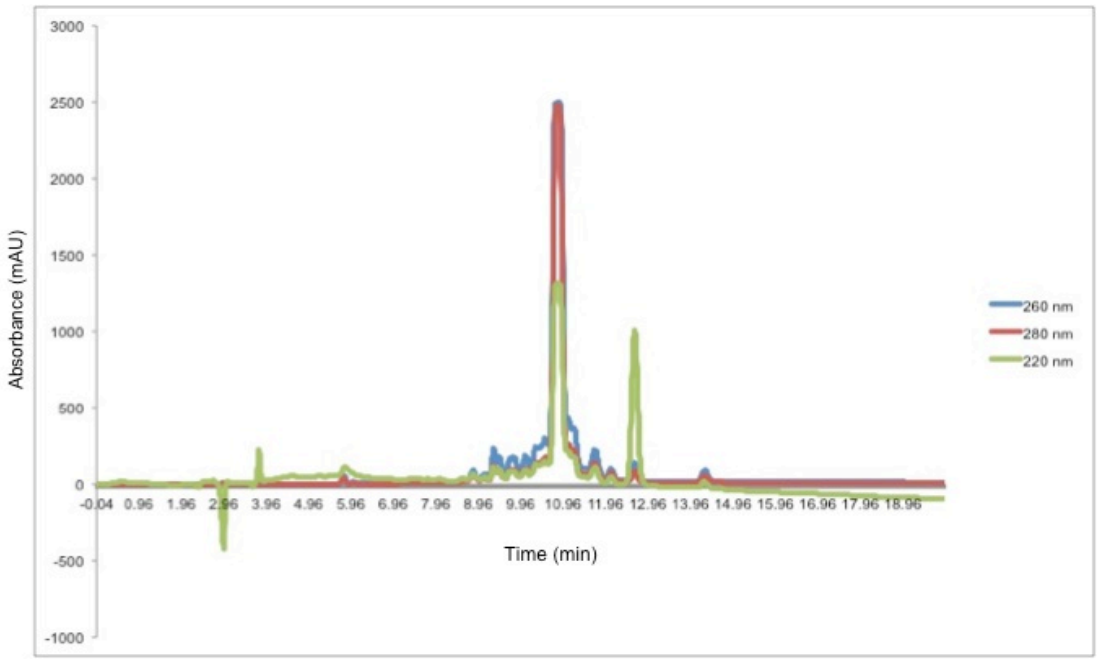

Figure 28: Characterization of dye-labeled CC61A'-Am single-stranded DNA using HPLC for the absorbance of DNA at 260 nm, 280 nm, and 220 nm. The largest peak corresponded to the unreacted DNA.

Table 2: Comparison of absorbances at 260 nm, 280 nm, and 220 nm for CC61A'-Am and cRGD-oligonucleotide reaction mixtures

		260 nm signal		280 nm signal		220 nm signal		Comparison ratios between areas of two signals	
	Time (min)	Area (mAU•s)	Height (mAU)	Area (mAU•s)	Height (mAU)	Area (mAU•s)	Height (mAU)	280/260	220/260
CC61A'-Am	10.85	40723.00	2487.41	34825.06	2473.28	24259.10	1451.46	0.86	0.60
pH 7.0, 1.5 hr	10.66	29069.54	2403.05	19753.76	1833.38	15377.48	1211.37	0.68	0.53
DMSO, 1.5 hr	10.79	17519.55	1950.32	10879.17	1246.72	9483.59	937.01	0.62	0.54
DMF, 1.5 hr	10.67	18501.13	2052.11	11756.50	1337.66	12467.79	1057.87	0.64	0.67
pH 7.0, 3.0 hr	11.06	14214.30	1465.10	8705.80	901.36	21432.85	1158.89	0.61	1.51
DMSO, 3.0 hr	11.13	18268.23	1942.11	11429.34	1244.45	17611.74	1105.44	0.63	0.96
DMF, 3.0 hr	10.86	16980.43	2165.42	10879.84	1455.78	10145.23	1067.13	0.64	0.60

Characterization of the interactions between cells and membrane-anchored DNA, cRGD and potential cRGD-oligonucleotides

In order to directly determine whether a cRGD-oligonucleotide conjugate was produced, HCC breast cancer cells were allowed to engage with functionalized supported lipid bilayers and were imaged using bright-field microscopy, reflection interference contrast microscopy (RICM), and fluorescence microscopy (Figure 29). As a negative control, cells were allowed to interact with membrane-anchored duplex CC61A-biotin/CC61A'-Cy3-Am DNA. Although, the cells were observed in the bright-field channel, adhesion to the surface was not seen in the RICM, demonstrating that dye-labeled duplex DNA could not mediate cell adhesion. Anchoring of the duplex DNA to the surface was seen as fluorescence from the Cy3 label in the TRITC channel. As a positive control, the cells were allowed to interact with the surface, on which biotinylated cRGD was incubated. In the bright-field channel, cells appeared to be spreading and engaging with the surface; in RICM, strong adhesion to the surface was observed. Moreover, a cell-like shape was seen in the Alexa 467 channel, suggesting that as the integrin receptors engaged the immobilized cRGD, the cell was clustering the peptides together. However, when allowed to interact with surfaces functionalized with the product of the cRGD-oligonucleotide conjugation reaction, the cells behaved as they did with the negative control surfaces; cells did not adhere to the surface as seen in the RICM. Furthermore, the dye-labeled streptavidin did not cluster into a cell-like shape. This suggested that the cRGD-oligonucleotide conjugate continued to remain elusive and may require new linking chemistry.

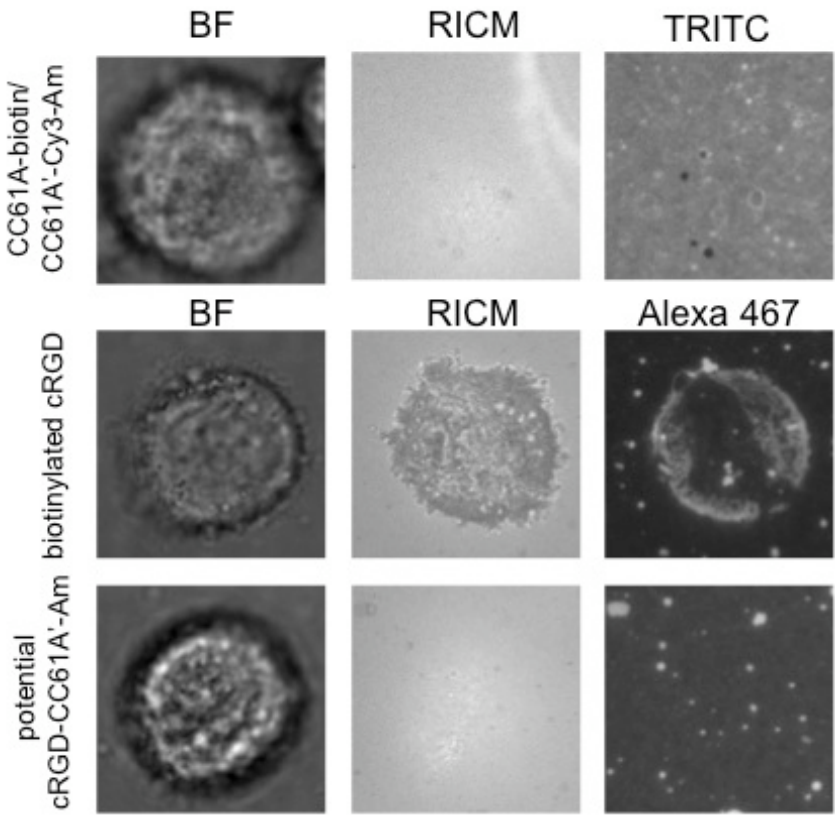

Figure 29: Interactions between cells and membrane-anchored DNA, cRGD and potential cRGD-oligonucleotides on supported lipid bilayers using bright-field microscopy, RICM and fluorescence. The membrane-anchored duplex CC61A-biotin/CC61A'-Cy3-Am DNA served as the negative control, while the biotinylated cRGD served as the positive control. The product of the cRGD-oligonucleotide conjugation reaction behaved similarly to the duplex DNA, suggesting that cRGD had not coupled to the oligonucleotide. (Each square represents an area of 27.7 μM × 27.7 μM.)

Conclusion

We have described the development of a self-healing and dynamic light responsive substrate to study the physical nature of integrin interactions with the cell adhesive peptide

RGD. Although the conjugation of a peptide to an oligonucleotide continues to need optimization, the selective release of the photocleavable duplex DNA with UV irradiation and the reversible recovery of the ligand have been clearly shown. Plans to use another type of coupling chemistry involving an acrydite functionalized oligonucleotide, CC61A'-Acryd, to the cysteine of cRGD-SH via a Michael addition have already been initiated. Upon successful conjugation of a cRGD peptide to an oligonucleotide, the effects of photo-triggered manipulation on cell adhesion can be investigated.

References

1. (a) Guillame-Gentil, O.; Semenov, O.; Roca, A. S.; Groth, T.; Zahn, R.; Voros, J.; Zenobi-Wong, M., Engineering the Extracellular Environment: Strategies for Building 2D and 3D Cellular Structures. *Advanced Materials* **2010,** *22* (48), 5443-5462; (b) Stevens, M. M.; George, J. H., Exploring and engineering the cell surface interface. *Science* **2005,** *310* (5751), 1135-1138.
2. (a) Groves, J. T.; Kuriyan, J., Molecular mechanisms in signal transduction at the membrane. *Nature Structural & Molecular Biology* **2010,** *17* (6), 659-665; (b) Scott, J. D.; Pawson, T., Cell Signaling in Space and Time: Where Proteins Come Together and When They're Apart. *Science* **2009,** *326* (5957), 1220-1224.
3. (a) DuFort, C. C.; Paszek, M. J.; Weaver, V. M., Balancing forces: architectural control of mechanotransduction. *Nature Reviews Molecular Cell Biology* **2011,** *12* (5), 308-319; (b) Hoffman, B. D.; Grashoff, C.; Schwartz, M. A., Dynamic molecular processes mediate cellular mechanotransduction. *Nature* **2011,** *475* (7356), 316-323.
4. (a) Arnaout, M. A.; Mahalingam, B.; Xiong, J. P., Integrin structure, allostery, and bidirectional signaling. *Annual Review of Cell and Developmental Biology* **2005,** *21*, 381-410; (b) Yu, C. H.; Law, J. B. K.; Suryana, M.; Low, H. Y.; Sheetz, M. P., Early integrin binding to Arg-Gly-Asp peptide activates actin polymerization and contractile movement that stimulates outward translocation. *Proceedings of the National Academy of Sciences of the United States of America* **2011,** *108* (51), 20585-20590.
5. (a) Petit, V.; Thiery, J. P., Focal adhesions: structure and dynamics. *Biology of the Cell* **2000,** *92* (7), 477-494; (b) Wozniak, M. A.; Modzelewska, K.; Kwong, L.; Keely, P. J., Focal adhesion regulation of cell behavior. *Biochimica Et Biophysica Acta-Molecular Cell Research* **2004,** *1692* (2-3), 103-119.
6. Hersel, U.; Dahmen, C.; Kessler, H., RGD modified polymers: biomaterials for stimulated cell adhesion and beyond. *Biomaterials* **2003,** *24* (24), 4385-4415.
7. Englund, E. A.; Wang, D.; Fujigaki, H.; Sakai, H.; Micklitsch, C. M.; Ghirlando, R.; Martin-Manso, G.; Pendrak, M. L.; Roberts, D. D.; Durell, S. R.; Appella, D. H., Programmable multivalent display of receptor ligands using peptide nucleic acid nanoscaffolds. *Nature Communications* **2012,** *3*, 614.
8. Auernheimer, J.; Dahmen, C.; Hersel, U.; Bausch, A.; Kessler, H., Photoswitched cell adhesion on surfaces with RGD peptides. *J. Am. Chem. Soc.* **2005,** *127* (46), 16107-16110.

9. Nakanishi, J.; Kikuchi, Y.; Takarada, T.; Nakayama, H.; Yamaguchi, K.; Maeda, M., Photoactivation of a substrate for cell adhesion under standard fluorescence microscopes. *Journal of the Americam Chemical Society* **2004,** *126* (50), 16314-16315.
10. Nakanishi, J.; Kikuchi, Y.; Inoue, S.; Yamaguchi, K.; Takarada, T.; Maeda, M., Spatiotemporal control of migration of single cells on a photoactivatable cell microarray. *Journal of the American Chemical Society* **2007,** *129* (21), 6694-+.
11. (a) Wirkner, M.; Alonso, J. M.; Maus, V.; Salierno, M.; Lee, T. T.; Garcia, A. J.; del Campo, A., Triggered Cell Release from Materials Using Bioadhesive Photocleavable Linkers. *Advanced Materials* **2011,** *23* (34), 3907-+; (b) Wirkner, M.; Weis, S.; San Miguel, V.; Alvarez, M.; Gropeanu, R. A.; Salierno, M.; Sartoris, A.; Unger, R. E.; Kirkpatrick, C. J.; del Campo, A., Photoactivatable caged cyclic RGD peptide for triggering integrin binding and cell adhesion to surfaces. *Chembiochem* **2011,** *12* (17), 2623-9.
12. Kloxin, A. M.; Kasko, A. M.; Salinas, C. N.; Anseth, K. S., Photodegradable Hydrogels for Dynamic Tuning of Physical and Chemical Properties. *Science* **2009,** *324* (5923), 59-63.
13. (a) Wildt, B.; Wirtz, D.; Searson, P. C., Programmed subcellular release for studying the dynamics of cell detachment. *Nature Methods* **2009,** *6* (3), 211-213; (b) Wildt, B.; Wirtz, D.; Searson, P. C., Triggering cell detachment from patterned electrode arrays by programmed subcellular release. *Nature Protocols* **2010,** *5* (7), 1273-1280.
14. Raghavan, S.; Desai, R. A.; Kwon, Y.; Mrksich, M.; Chen, C. S., Micropatterned dynamically adhesive substrates for cell migration. *Langmuir* **2010,** *26* (22), 17733-8.
15. (a) Nair, P. M.; Salaita, K.; Petit, R. S.; Groves, J. T., Using patterned supported lipid membranes to investigate the role of receptor organization in intercellular signaling. *Nature Protocols* **2011,** *6* (4), 523-539; (b) Chan, Y. H. M.; Boxer, S. G., Model membrane systems and their applications. *Current Opinion in Chemical Biology* **2007,** *11* (6), 581-587.
16. Salaita, K.; Nair, P. M.; Petit, R. S.; Neve, R. M.; Das, D.; Gray, J. W.; Groves, J. T., Restriction of Receptor Movement Alters Cellular Response: Physical Force Sensing by EphA2. *Science* **2010,** *327* (5971), 1380-1385.
17. Patwa, A.; Gissot, A.; Bestel, I.; Barthelemy, P., Hybrid lipid oligonucleotide conjugates: synthesis, self-assemblies and biomedical applications. *Chemical Society Reviews* **2011,** *40* (12), 5844-5854.
18. Chan, Y. H.; van Lengerich, B.; Boxer, S. G., Effects of linker sequences on vesicle fusion mediated by lipid-anchored DNA oligonucleotides. *Proceedings of the National Academy of Sciences of the United States of America* **2009,** *106* (4), 979-84.
19. Loew, M.; Springer, R.; Scolari, S.; Altenbrunn, F.; Seitz, O.; Liebscher, J.; Huster, D.; Herrmann, A.; Arbuzova, A., Lipid Domain Specific Recruitment of Lipophilic Nucleic Acids: A Key for Switchable Functionalization of Membranes. *Journal of the American Chemical Society* **2010,** *132* (45), 16066-16072.
20. Thompson, M. P.; Chien, M. P.; Ku, T. H.; Rush, A. M.; Gianneschi, N. C., Smart Lipids for Programmable Nanomaterials. *Nano Letters* **2010,** *10* (7), 2690-2693.
21. (a) Olejnik, J.; KrzymanskaOlejnik, E.; Rothschild, K. J., Photocleavable biotin phosphoramidite for 5'-end-labeling, affinity purification and phosphorylation of synthetic oligonucleotides. *Nucleic Acids Research* **1996,** *24* (2), 361-366; (b) Hasan, A.; Stengele, K. P.; Giegrich, H.; Cornwell, P.; Isham, K. R.; Sachleben, R. A.; Pfleiderer, W.; Foote, R. S., Photolabile protecting groups for nucleosides: Synthesis and photodeprotection rates. *Tetrahedron* **1997,** *53* (12), 4247-4264.
22. (a) Beaucage, S. L.; Iyer, R. P., Advances in the Synthesis of Oligonucleotides by the Phosphoramidite Approach. *Tetrahedron* **1992,** *48* (12), 2223-2311; (b) Eritja, R., Solid-phase synthesis of modified oligonucleotides. *International Journal of Peptide Research and Therapeutics* **2007,** *13* (1-2), 53-68.
23. (a) Williams, B. A.; Chaput, J. C., Synthesis of peptide-oligonucleotide conjugates using a heterobifunctional crosslinker. *Current Protocols in Nucleic Acid Chemistry* **2010,** *Chapter 4*,

Unit4 41; (b) Tournier, E. J. M.; Wallach, J.; Blond, P., Sulfosuccinimidyl 4-(N-maleimidomethyl)-1-cyclohexane carboxylate as a bifunctional immobilization agent. Optimization of the coupling conditions. *Anal. Chim. Acta* **1998,** *361* (1-2), 33-44.
24. Hermanson, G. T., *Bioconjugate techniques*. 2nd ed.; Elsevier ;
Academic Press: Amsterdam ; Boston
London ; Burlington, MA, 2008; p xxx, 1202 p.
25. Gangar, A.; Fegan, A.; Kumarapperuma, S. C.; Wagner, C. R., Programmable self-assembly of antibody-oligonucleotide conjugates as small molecule and protein carriers. *Journal of the American Chemical Society* **2012,** *134* (6), 2895-7.
26. Lapienc, V.; Kukolka, F.; Kiko, K.; Arndt, A.; Niemeyer, C. M., Conjugation of Fluorescent Proteins with DNA Oligonucleotides. *Bioconjugate Chemistry* **2010,** *21* (5), 921-927.